

# Optimal transport over nonlinear systems via infinitesimal generators on graphs

Karthik Elamvazhuthi\*      Piyush Grover<sup>†</sup>

January 22, 2024

## Abstract

We present a set-oriented graph-based computational framework for continuous-time optimal transport over nonlinear dynamical systems. We recover provably optimal control laws for steering a given initial distribution in phase space to a final distribution in prescribed finite time for the case of non-autonomous nonlinear control-affine systems, while minimizing a quadratic transport cost. The resulting control law can be used to obtain approximate feedback laws for individual agents in a swarm control application. Using infinitesimal generators, the optimal control problem is reduced to a modified Monge-Kantorovich optimal transport problem, resulting in a convex Benamou-Brenier type fluid dynamics formulation on a graph. The well-posedness of this problem is shown to be a consequence of the graph being strongly-connected, which in turn is shown to result from controllability of the underlying dynamical system. Using our computational framework, we study optimal transport in dynamical systems arising in chaotic fluid dynamics and non-holonomic vehicle dynamics. The solutions to the optimal transport problem elucidate the role played by invariant manifolds, lobe-dynamics and almost-invariant sets in efficient transport of distributions in finite time. Our work connects set-oriented operator-theoretic methods in dynamical systems with optimal mass transportation theory, and opens up new directions in design of efficient feedback control strategies for nonlinear multi-agent and swarm systems operating in nonlinear ambient flow fields.

## 1 Introduction

Understanding, computing and controlling phase space transport is of utmost importance in the study of nonlinear dynamical systems. For computation of phase space transport

---

\*Arizona State University, Tempe, AZ, USA

<sup>†</sup>Mitsubishi Electric Research Labs, Cambridge, MA, USA. Corresponding Author. Email: grover@merl.com

This work was solely funded by Mitsubishi Electric Research Labs.

in dynamical systems, the available techniques can be divided into roughly three classes: geometric, topological and statistical (or operator theoretic) methods.

The geometric methods, originating in Poincaré’s [1] work in celestial mechanics, aim at extracting structures in phase space that organize transport. In recent years, the focus in this field has been on extracting the Lagrangian coherent structures in autonomous and non-autonomous systems, which are often the stable and unstable manifolds [2] of fixed points or periodic orbits, or their time-dependent analogues [3]. Related techniques based on lobe-dynamics [2] allow for quantifying transport between different weakly mixing regions in the phase space. Application to low-dimensional systems arising in fluid kinematics [4, 5], celestial mechanics [6], and plasma physics [7] have been developed over the years. Once these Lagrangian structures have been identified, intelligent control strategies can be formulated to obtain efficient phase space transport between the desired regions in the phase space; see Refs. [6, 8, 9, 10, 11] for some recent work in this area. The topological methods, based on the idea of ‘topological forcing’ [12], provide rigorous bounds and sharp estimates of certain transport related quantities. For example, such methods have been applied in the study of passive scalar mixing in laminar fluid flows [13, 14]. Some topological optimal control problems have also been studied [15].

Operator-theoretic statistical techniques [16] are based on lifting the evolution from the state space to the space of measures, in case of the Perron-Frobenius (or transfer) operator, and to the space of observables, in case of the Koopman operator. In both cases, the resulting (uncontrolled) dynamical system is linear, albeit in infinite dimensions. The linearity allows for immediate application of techniques from linear algebra and linear systems theory. Numerical methods based on operator theory have been developed, and applied to several problems of contemporary interest [17, 18, 19, 20, 21]. Recent work has also shown that combining the statistical methods with geometric [22, 23, 24], or topological methods [25, 26] can give further qualitative and quantitative information about phase space transport. The set-oriented numerical methods for computing transfer operators [18, 20] are especially promising. Using efficient phase space discretization techniques, these methods enable discovery of ‘coherent sets’ in autonomous [27] and non-autonomous [28] dynamical systems.

In this paper, we develop a set-oriented framework for the problem of continuous-time ‘optimal transport’ [29] of phase space measure under controlled nonlinear dynamics. This problem involves optimally steering an initial measure on a phase space  $X$ , to a final measure in given finite time. Specifically, we consider nonlinear control-affine systems of the form,

$$\dot{x}(t) = g_0(x(t), t) + \sum_{i=1}^n u_i(t) g_i(x(t)). \quad (1)$$

Our aim is to compute controls  $u_i$  such that a cost of transporting a measure  $\mu_{t_0}$  to  $\mu_{t_f}$  over the time-horizon  $[t_0, t_f]$  is minimized. This cost is given by the integral over phase-space and time,

$$C = \int_X \int_{t_0}^{t_f} |u(x, t)|^2 dt d\mu(x). \quad (2)$$

A major motivation for studying this problem comes from the field of multi-agent systems or swarm control. The problem of path planning and control of a swarm of homogenous agents in an ambient nonlinear flow field can be formulated as optimal transport problem in the presence of nonlinear dynamics. For instance, the control of magnetic particles in blood stream [30, 31, 32], robotic bees in air [33, 34], and swarms of autonomous underwater vehicles (AUVs) in the ocean [35] can all be studied in this setting. Here, one represents the distribution of swarms in phase space by measures. The solution of this control problem provides an open-loop control for the measure, and an approximate feedback control for individual agents, to move from an initial to final measure in finite time.

This problem also arises naturally in the realm of nonlinear control systems of a single ‘agent’, where its initial and final states can only be specified as probability distributions. In this case, the measures involved are probability measures, and hence, the optimal transport cost  $C$  is the *expectation* of control cost over all possible initial and final states.

## 1.1 Set-Oriented Methods in Trajectory Planning and Control

The setting of set-oriented methods is especially well-suited for development of rigorous methods for controlling phase space transport in various settings. For example, optimal control algorithms using set-oriented methods have been developed [36, 37, 38]. Other related work was pursued in Refs. [39, 40, 41], where an optimal control framework for asymptotic feedback stabilization of arbitrary initial measure to an attractor is presented. This framework is based on computing a (control) ‘Lyapunov measure’, which is a measure-theoretic analogue of control Lyapunov function. Also relevant is the work in the area of occupation measures, see Ref. [42]. We also note that set-oriented transfer-operator and infinitesimal generator based methods have been used in optimal control of mixing passive scalars in fluids, see Refs. [43, 44].

## 1.2 Optimal Transport

The field of optimal mass transportation [29] is concerned with optimal mapping of measures in different settings, including on graphs [45], and has deep connections with phase space transport in dynamical systems [46, 47, 48]. The problem of optimal transport in linear dynamical systems has been studied recently [49, 50, 51], resulting in several theoretical and computational advances. In previous related work of the authors [52], a computational method to obtain optimal discrete-time perturbations which result in desired measure transport under nonlinear dynamics in finite time was presented. The discrete-time perturbations were obtained by solving a Monge-Kantorovich optimal transport problem on graphs in *pseudo-time*. The ‘control’ perturbations were modeled as instantaneous, and full controllability was assumed.

### 1.3 Contributions

We develop a set-oriented graph-based computational framework for continuous-time optimal transport over nonlinear dynamical systems of the form given in Eq. (1). The solution of this problem provides an open-loop control for the measure, and an approximate feedback control for individual agents, to move from an initial to final measure in finite time. Using infinitesimal generators, the optimal control problem is reduced to a modified Monge-Kantorovich optimal transport problem, resulting in a convex Benamou-Brenier type fluid dynamics formulation on a graph. We show that the well-posedness of the controlled optimal transport problem on this graph is related to controllability of the underlying dynamical system. We prove that if the underlying dynamical system is controllable, the graph obtained in our formulation is strongly-connected. It is then proved that arbitrary final measures not lying on the boundary of the probability simplex can be reached in finite-time.

Using this framework, we compute optimal transport in systems related to chaotic fluid dynamics and non-holonomic vehicle dynamics. The application to periodically driven double-gyre rigorously elucidates the role of invariant manifolds, lobe-dynamics and almost-invariants sets in efficient finite-time transport of distributions in the phase space.

## 2 Background and Mathematical Preliminaries

The development of our computational framework in Section 3 uses concepts from control systems theory, optimal transport and set-oriented numerical methods. We briefly review the relevant topics in this section, and introduce the required mathematical notation and constructions. Along the way, we motivate the developments of Section 3 by relating the continuous and discrete (graph-based) concepts of optimal transport over dynamical systems.

### 2.1 Monge-Kantorovich Problem and Benamou-Brenier Approach

The Monge-Kantorovich optimal transport (OT) problem [29] is concerned with mapping of an initial measure  $\mu_0$  on a space  $X$  to a final measure  $\mu_1$  on a space  $Y$ . In the original formulation, it involves solving for a measurable transport map  $T : X \rightarrow Y$ , which pushes forward  $\mu_0$  to  $\mu_1$  in an optimal manner. The cost of transport per unit mass is prescribed by a function  $c(x, T(x))$ . Hence, the optimization problem is

$$\begin{aligned} \inf_T \int c(x, T(x)) d\mu_0(x), \\ \text{s.t. } T_{\#}\mu_0 = \mu_1, \end{aligned} \tag{3}$$

where  $T_{\#}$  is the pushforward of  $T$ , i.e.  $(T_{\#}\mu)(A) = \mu(T^{-1}(A))$  for every  $A$ . The pushforward constraint in this problem makes the optimization problem highly nonlinear and non-convex. The existence and uniqueness of optimal solutions for various settings has been major topic of research. In a ‘relaxed’ version of this problem, due to Kantorovich, the optimization problem is to obtain an optimal joint distribution  $\pi(X \times Y)$  on the product space  $X \times Y$ ,



where the marginal of  $\pi$  on  $X$  is  $\mu_0$  and on  $Y$  is  $\mu_1$ . We denote by  $\prod(\mu_0, \mu_1)$  the set of all measures on product space with the marginals  $\mu_0$  and  $\mu_1$  on  $X$  and  $Y$  respectively. Hence, the relaxed problem is

$$\inf_{\pi(X \times Y) \in \prod(\mu_0, \mu_1)} \int c(x, y) d\pi(x, y) \quad (4)$$

For the case of quadratic costs, i.e.,  $c(x, y) = \|x - y\|^2$ , the support of the optimal distribution  $\pi(X \times Y)$  is the graph of the optimal map  $T$  obtained from the solution of problem 3. The square-root of the optimal cost obtained as solution of this problem is called the 2-Wasserstein distance, and we denote it by  $W_2(\mu_0, \mu_1)$ . We concern ourselves with only quadratic cost in this paper.

A major conceptual and computational breakthrough in the optimal transport theory was the development of fluid dynamical interpretation of OT problem by Brenier-Benamou [53]. This work provides the first connection of OT with dynamical systems, and evolution equations in general. The OT problem in Eq. (3) is concerned with only the initial and final measures. The optimal map  $T$  in the quadratic cost case is known to be of the form  $T(x) = \nabla\psi(x)$  for some convex function  $\psi(x)$ . Then, the pushforward constraint can be written as,

$$\det(D^2\psi(x))\mu_1(\nabla\psi(x)) = \mu_0(x), \quad (5)$$

where  $D^2$  is the Hessian. Numerically solving the optimization problem with nonlinear constraint given in Eq. (5) is difficult. The fluid dynamical approach, first developed in Ref. [53], provides a more tractable way to the solution of this problem. In this approach, the optimization problem is formulated in terms of an advection field  $u(x, t)$ , and initial and final *densities*  $(\rho_0(x), \rho_1(x))$  of a passive scalar. The core idea is to obtain the optimal map  $T$  as a result of advection over a ‘time’ period  $(t_0, t_f)$  by an optimal advection field  $u(x, t)$ . It can be shown that the optimization problem given by Eq. (3) (with  $X = Y = \mathbb{R}^d$ ) with quadratic cost is equivalent to the following problem:

$$W_2^2(\mu_0, \mu_1) = \inf_{u(x, t), \rho(x, t)} \int_{\mathbb{R}^d} \int_{t_0}^{t_f} \rho(x, t) |u(x, t)|^2 dt dx \quad (6)$$

$$\begin{aligned} \text{s.t. } & \frac{\partial \rho(x, t)}{\partial t} + \nabla \cdot (\rho(x, t)u(x, t)) = 0 \\ & \rho(x, t_0) = \rho_0(x), \rho(x, t_f) = \rho_1(x) \end{aligned} \quad (7)$$

This aim of this problem can be understood as minimizing the time integral of the total kinetic energy of the ‘fluid’ being advected with velocity field  $u(x, t)$ , subjected to initial and final densities of the passive scalar. The motion of a passive scalar is governed by the ordinary differential equation

$$\dot{x}(t) = u(x, t). \quad (8)$$

Furthermore, the optimal advection field is a potential flow, i.e.,  $u(x, t) = \nabla\phi(x, t)$  for some potential field  $\phi(x, t)$ . The Euler-Lagrange equations for this optimization problem can be written as

$$\frac{\partial\phi}{\partial t} + \frac{|\nabla\phi|^2}{2} = 0, \quad (9)$$

which are pressure-less version of Euler equations.

By a change of variables from  $(\rho, u)$  to  $(\rho, m \triangleq \rho u)$ , the optimization problem in Eq. (17) can be put into a form where its convexity can be proved easily. The transformed optimization problem is

$$\begin{aligned} & \inf_{\rho(x,t) \geq 0, m(x,t)} \int_{\mathbb{R}^d} \int_{t_0}^{t_f} \frac{|m(x, t)|^2}{\rho(x, t)} dt dx, \\ \text{s.t. } & \frac{\partial\rho(x, t)}{\partial t} + \nabla \cdot (m(x, t)) = 0, \quad t_0 \leq t \leq t_f, \\ & \rho(x, t_0) = \rho_0(x), \rho(x, t_f) = \rho_1(x). \end{aligned} \quad (10)$$

In the above equations, the constraints are now linear in the problem variables  $(\rho, m)$ . The term inside the integral in the cost function,  $\frac{|m(x, t)|^2}{\rho(x, t)}$ , is of the ‘quadratic-over-linear’ form, and can be shown to be convex. Hence, by transforming the transport problem into continuous time, and by using a change of variables, the non-convex problem in Eq. (3) has been converted into a convex problem in Eq. (10).

## 2.2 Optimal Transport in Controlled Dynamical Systems

Next, we discuss the generalization of the optimal transport problem on continuous spaces to general nonlinear controlled dynamical systems, following Refs. [54, 50]. Consider the following system for  $x \in \mathbb{R}^d$ ,

$$\dot{x}(t) = f(x(t), u(t)). \quad (11)$$

The problem of optimal transport for this system can be posed as finding optimal control which steers an initial scalar density to a final density, where the scalar transport occurs due to combination of an ambient flow field  $f(x(t), 0)$ , and control  $u(t)$ . This problem can be posed by replacing the cost function  $c$  with a Lagrangian representing the optimal control cost i.e.,

$$c(x_1, x_2) = \inf_{\mathbb{U}_{x_1}^{x_2}} \int_{t_0}^{t_f} L(t, x(t), u(t)) dt, \quad (12)$$

$$x(t_0) = x_1, x(t_f) = x_2 \quad (13)$$

under the constraint given by evolution Eq. (11), and where  $\mathbb{U}_{x_1}^{x_2}$  is the set of admissible controls that drive the system given in Eq (11) from  $x(t_0) = x_1$  to  $x(t_f) = x_2$ . The existence and regularity of the corresponding optimal transport problem has been studied in recent literature [54, 46, 55], computation of transport maps for general nonlinear systems is a difficult problem. For the special case of linear dynamical systems with quadratic cost, mirroring the optimal control case, further analytical development and computational simplification has been made [49, 50]. As described in Ref. [50], consider the following setup:

$$c(x_1, x_2) = \inf_{\mathbb{U}_{x_1}^{x_2}} \int_{t_0}^{t_f} \frac{1}{2} \|u\|^2 dt, \quad (14)$$

$$\dot{x}(t) = A(t)x(t) + B(t)u(t), \quad t_0 \leq t \leq t_f, \quad (15)$$

$$x(t_0) = x_1, x(t_f) = x_2. \quad (16)$$

The generalization of Benamou-Brenier approach to the corresponding optimal transport problem can be seen to be the following:

$$\begin{aligned} & \inf_{u(x,t), \rho(x,t)} \int_{\mathbb{R}^d} \int_{t_0}^{t_f} \rho(x, t) |u(x, t)|^2 dt dx, \quad (17) \\ \text{s.t. } & \frac{\partial \rho(x, t)}{\partial t} + \nabla \cdot ((A(t)x(t) + B(t)u(x, t))\rho(x, t)) = 0, \quad t_0 \leq t \leq t_f, \\ & \rho(x, t_0) = \rho_0(x), \rho(x, t_f) = \rho_1(x). \end{aligned}$$

We note that the optimal transport problem given by Eq. (17) can also be interpreted as the problem of optimally steering a dynamical system from a probabilistic initial state to a probabilistic final state. Note that the dynamics of the system are still taken to be deterministic; however see Ref. [51] for connections with stochastic dynamical systems.

The linearity of dynamics allows significant simplification of the analysis. Analytical solutions to the optimal transport problem for the case of Gaussian initial and final measures were derived in Ref. [50]. For the purpose of studying measure transport in nonlinear systems, we use tools from operator theory, which are discussed next.

## 2.3 Transfer Operator and Infinitesimal Generator

Consider the flow-map  $\phi_{t_0}^{t_0+T} : X \rightarrow X$  on a  $d$ -dimensional phase space  $X$ . This map may be obtained as a time- $T$  map of the flow of a possibly time-dependent dynamical system,

$$\dot{x} = f(x, t). \quad (18)$$

The corresponding Perron-Frobenius transfer operator [16]  $P_{t_0}^{t_0+T}$  is a linear operator which pushes forward measures in phase space according to the dynamics of the trajectories under  $\phi_{t_0}^{t_0+T}$ . Let  $\mathbf{B}(X)$  denote  $\sigma$ -algebra of Borel sets in  $X$ . Then, for any measure  $\mu$ ,

$$P_{t_0}^{t_0+T} \mu(A) = \mu((\phi_{t_0}^{t_0+T})^{-1}(A)) \quad \forall A \in \mathbf{B}(X). \quad (19)$$

The transfer operator lifts the evolution of the dynamical systems from phase space  $X$  to the space of measures  $\mathbf{M}(X)$ . Numerical approximation of  $P$ , denoted by  $\hat{P}$ , may be viewed as a transition matrix of an  $N$ -state Markov chain [20]. For computation, we partition the phase space volume of interest into  $N$   $d$ -dimensional connected, positive volume subsets,  $B_1, B_2, \dots, B_N$  with piecewise smooth boundaries  $\partial B_i$ . Usually, these subsets are hyper-rectangles. The matrix  $\hat{P} = \{\hat{p}_{ij}\}$  is numerically computed via the Ulam-Galerkin method [56, 20], as follows

$$\hat{p}_{ij} = \frac{\bar{m}((\phi_{t_0}^{t_0+T})^{-1}(B_i) \cap B_j)}{\bar{m}(B_j)}, \quad (20)$$

where  $\bar{m}$  is the Lebesgue measure. The action of the transfer operator over a finite time  $T$  can also be defined naturally on densities in the case of Lebesgue absolutely continuous measures. However, we are more interested in capturing the continuous-time behavior of the dynamical system in Eq. (18) in the space of densities. The continuity equation for system in Eq. (18), is given by

$$\frac{d\mu}{dt} = -\nabla \cdot (f(x, t)\mu). \quad (21)$$

For the numerical approach used in this paper we briefly consider the Eq. (21), in a operator theoretic framework, as an abstract ordinary differential equation in the space of measures, formally. Eq. (21) can be expressed as

$$\dot{\mu}(t) = \mathcal{A}(t)\mu ; \quad \mu(s) = \mu_s \in \mathbf{M}(X), \quad (22)$$

where  $\mathcal{A}(t) : D(\mathcal{A}(t)) \rightarrow \mathbf{M}(X)$ ,  $D(\mathcal{A}(t)) \subset \mathbf{M}(X)$  and the solution,  $\mu(t)$ , of Eq. (22) can be expressed using a two-parameter semigroup of operators  $(\mathcal{U}(t, s))_{s, t \in \mathbb{R}, t \geq s}$  as  $\mu(t) = \mathcal{U}(t, s)\mu_s$ . The divergence operation is to be understood in the sense of duality of  $M(X)$  with  $C(X)$  (assuming  $X$  is compact). Here  $C(X)$  refers to the space of continuous functions on  $X$ . The Perron-Frobenius operator is related to this two-parameter semigroup of operators as  $\mathcal{U}(T, t_0) = P_{t_0}^{t_0+T}$  for given parameters  $t_0$  and  $T$ . In general, guaranteeing the existence of a strongly continuous two-parameter semigroup based on the time-dependent generator  $\mathcal{A}(t)$  is quite involved. See for example Refs. [57, 58]. In contrast, the theory is more well-developed for the case when  $\mathcal{A}(t) \equiv \mathcal{A}$ , (the vector field  $f(\mathbf{x})$  is time independent). In this case, the solution,  $\mu(t)$ , can be expressed by a one-parameter semigroup of bounded operators,  $(\mathcal{T}(t))_{t \geq 0}$ , as  $\mu(t) = \mathcal{T}(t-s)\mu_s$ . Here, the generator  $\mathcal{A}$  and  $\mathcal{T}(t)$  are related by the formula

$$\mathcal{A}\mu = \lim_{h \rightarrow 0^+} \frac{\mathcal{T}(h)\mu - \mu}{h} \text{ for each } \mu \in D(\mathcal{A}). \quad (23)$$

As in the case of the Perron-Frobenius operator, one can also consider the semigroup and its generator on a space of densities (or equivalently on a space of measures absolutely continuous with respect to a reference measure with additional regularity restrictions).

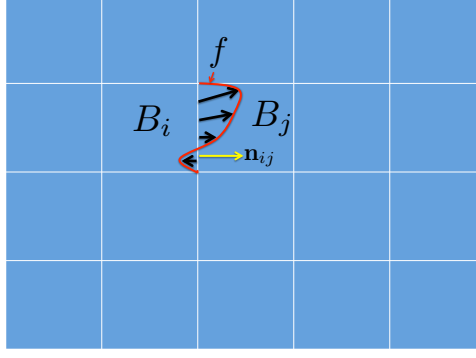


**Figure 1:** Computation of infinitesimal generator  $F$ . The entry  $F_{ij}$  is proportional to flux across  $B_i \cap B_j$  from  $B_i$  to  $B_j$ , due to vector field  $f$ .

Ulam's method for approximating Perron-Frobenius operators using Markov matrices extends to numerical approximations of semigroups corresponding to the continuity equation. Analogously, one approximates the generator of the semigroup using transition rate matrices, which generate approximating semigroups on a finite state space. We recall this method as shown in [59]. We denote by  $\bar{B}_i$  the closure of  $B_i$ . The operator  $\mathcal{A}(t)$  is approximated by defining elements of time-varying transition rate matrix  $\{A_{ij}(t)\}$ , which are computed as follows,

$$A_{ij}(t) = \begin{cases} \frac{1}{\bar{m}(B_j)} \int_{\bar{B}_i \cap \bar{B}_j} \max\{f(x, t) \cdot \mathbf{n}_{ij}, 0\} & i \neq j, \\ -\sum_{k \neq i} \frac{\bar{m}(\bar{B}_k)}{\bar{m}(\bar{B}_i)} A_{ik}(t) & \text{otherwise,} \end{cases} \quad (24)$$

where  $\mathbf{n}_{ij}$  is the unit normal vector pointing out of  $B_i$  into  $B_j$  if  $\bar{B}_i \cap \bar{B}_j$  is a  $(d-1)$  dimensional face, and zero vector otherwise. See Fig. 1. Note that in [59], the authors also considered the perturbed version of the operator,  $-\nabla \cdot (f(x, t) \cdot) : -\nabla \cdot (f(x, t) \cdot) + \frac{\epsilon^2}{2} \Delta$ . This was mainly to exploit the spectral properties of the perturbed operator and the corresponding semigroup. However, in this work the perturbed operator does not offer any visible advantages. Hence, we work with approximations of the operator,  $-\nabla \cdot (f(x, t) \cdot)$ , alone. Nevertheless, we note that the discretization will introduce some numerical diffusion.

## 2.4 Monge-Kantorovich Transport on Graphs

Now consider a directed graph  $\mathcal{G} = (\mathcal{V}, \mathcal{E})$  on  $X$ , where the set of vertices  $\mathcal{V}$  represent the subsets  $B_i$  as before, and the set of directed edges  $\mathcal{E}$  are obtained from the topology of  $X$ . For each pair of neighboring vertices, two edges are constructed, one in each direction.

A continuous-time advection on such a graph can be described [60, 61] as,

$$\frac{d}{dt} \mu(t, v) = \sum_{e=(w \rightarrow v)} U(t, e) \mu(t, w) - \sum_{e=(v \rightarrow w)} U(t, e) \mu(t, v), \quad (25)$$

where  $\mu(t, v)$  is the time-varying measure on a vertex  $v$ , and  $U(t, e)$  is the flow on an edge  $e$ . Here we use the notation  $e = (v \rightarrow w)$  to represent the edge  $e$  directed from a vertex  $v$  to  $w$ . The notion of optimal transport has been extended to such a continuous-time discrete-space setting recently [45, 62, 63, 64]. Following [64], one can formulate a quadratic cost optimal transport problem on  $\mathcal{G}$  as follows. First, define an advective inner product between two flows  $U_1, U_2$  as

$$\langle U_1, U_2 \rangle_\mu = \sum_{e=(v \rightarrow w)} \left( \frac{\mu(v)}{\mu(w)} \cdot \frac{\mu(v) + \mu(w)}{2} \right) U_1(e) U_2(e). \quad (26)$$

Then the corresponding optimal transport distance between a set of measures  $(\mu_0, \mu_1)$  supported on  $V$  can be written as

$$\begin{aligned} \tilde{W}_N(\mu_0, \mu_1) = \inf_{\substack{U(t,e) \geq 0, \mu(t,v) \geq 0 \\ \text{such that Eq (25) holds, and} \\ \mu(0,v) = \mu_0(v), \mu(1,v) = \mu_1(v) \quad \forall v \in V.}} \int_0^1 \|U(t, \cdot)\|_{\mu(t, \cdot)} dt, \end{aligned} \quad (27)$$

Here  $\|U(t, \cdot)\|_{\mu(t, \cdot)} \triangleq \sqrt{\langle U, U \rangle_\mu}$ . This approach is motivated by the previously discussed Benamou-Brenier approach for optimal transport on continuous spaces, and results in the following advection based convex optimization problem.

$$\tilde{W}_N(\mu_0, \mu_1)^2 = \inf_{J(t,e) \geq 0, \mu(t,v) \geq 0} \int_0^1 \sum_{e=(v \rightarrow w)} \frac{J(t, e)^2}{2} \left( \frac{1}{\mu(t, v)} + \frac{1}{\mu(t, w)} \right) dt, \quad (28)$$

$$\mu(0, v) = \mu_0(v), \mu(1, v) = \mu_1(v) \quad \forall v \in V, \quad (29)$$

$$\frac{d}{dt} \mu(t, \cdot) = D^T J(t, \cdot), \quad (30)$$

where  $J(t, e) \triangleq \mu(t, v) U(t, e)$  for  $e = (v \rightarrow w)$ , and  $D \in \mathbb{R}^{|\mathcal{E}| \times |\mathcal{V}|}$  is the linear flow operator computing  $\mu(w) - \mu(v)$  for each  $e = (v \rightarrow w) \in \mathcal{E}$ . Specifically,  $D^T(i, j)$  equals +1 if  $j$ th edge points into  $i$ th vertex, -1 if  $j$ th edge points out of  $i$ th vertex, and 0 if  $j$ th edge is not connected to  $i$ th vertex. Hence Eq. (30) is a rewriting of Eq. (25) in terms of  $J(t, \cdot)$ . The change of variables from  $U$  to  $J$  is analogous to the change of variables in Brenier-Benamou formulations, as discussed earlier in this section.

The convergence of  $\tilde{W}_N$  to  $W_2$ , the 2-Wasserstein distance on a continuous phase space (a  $d$ -torus), as  $N \rightarrow \infty$  is studied in Ref. [62]. The convergence analysis is performed by constructing discrete measures over cubes, and discrete vector fields by integration of flow over boundaries (called ‘momentum vector fields’). This process is analogous to the above mentioned construction of discrete measures on  $\mathcal{V}$ , and representation of flow by edge-based variable  $J$ . While the aim of that paper is to show convergence of a different distance (denoted  $W_N$ ) to  $W_2$ , the distance  $\tilde{W}_N$  is used as an intermediate measure. It is shown that for absolutely continuous measures,  $\exists \delta > 0$  s.t. for any  $N > 0, \epsilon > 0$ ,

$$\frac{1}{c\sqrt{d}} W_N(\mu_0, \mu_1) \leq W_2(\mu_0, \mu_1) \leq \tilde{W}_N(\mu_0, \mu_1) \leq (1 + z(\delta, N))(W_N(\mu_0, \mu_1) + \epsilon),$$

where  $z(\delta, N) = o(\frac{\delta^2}{N})$ . Here we have abused notation by using  $(\mu_0, \mu_1)$  for measures in both continuous and discrete spaces. The constant  $c$  is independent of discretization. The convergence of  $\tilde{W}_N$  follows by a simple sandwiching argument. We drop the subscript  $N$  in the rest of the paper.

**Continuous-Discrete Analogy:** Conceptually, one can regard the problem described by Eqs. (28-30) as the graph-based analogue of the optimal transport problem given in Eq. (10). Recall that this corresponds to *single-integrator dynamics*  $\dot{x} = u(t)$ . In the next section, we use this interpretation, and generalize this graph-based framework to nonlinear dynamical systems of the form given in Eq. (1).

### 3 Problem Setup and Computational Approach

#### 3.1 Formulation of Optimal Transport Problem on Graphs

Let  $M \subset \mathbb{R}^d$  be an open bounded connected subset of an Euclidean space with piecewise smooth boundary. For a collection of analytic time-invariant vector fields  $\{g_i\}_{i=1}^n$  and possibly time-varying vector field  $g_0$  on  $M$ , consider the control affine system of the form

$$\begin{aligned} \dot{x}(t) &= g_0(x(t), t) + \sum_{i=1}^n u_i(t) g_i(x(t)) \\ x(0) &= x_0 \end{aligned} \quad (31)$$

Then given the densities  $\rho_0$  and  $\rho_1$  on  $M$ , the corresponding optimal transport problem of interest is the following

$$\inf_{u(x,t), \rho(x,t)} \int_{\mathbb{R}^n} \int_{t_0}^{t_f} \rho(x, t) |u_i(x, t)|^2 dt dx, \quad (32)$$

$$\text{s.t. } \frac{\partial \rho(x, t)}{\partial t} + \nabla \cdot (\rho(x, t) g_0(x, t)) + \sum_{i=1}^n \nabla \cdot (\rho(x, t) u_i(x, t) g_i(x)) = 0 \quad x \in M, \quad (33)$$

$$\begin{aligned} \vec{n} \cdot (g_0(x, t) \rho(x, t) + \sum_{i=1}^n u_i(x, t) g_i(x) \rho(x, t)) &= 0 \quad a.e. \quad x \in \partial M, \\ \rho(x, 0) &= \rho_0(x), \rho(x, 1) = \rho_1(x). \end{aligned}$$

Here,  $\vec{n}$  is the outward normal vector at the boundary of  $M$ , and we have assumed zero mass flux boundary conditions.

We approximate the optimal transport problem using a sequence of optimal transport problems on graphs. A key tool is to approximate the (time-varying) generator of the semigroup corresponding to the Eq. (33) using generator approximations on a finite state space as described in [59] and briefly discussed in Section 2.3. Hence, we approximate solutions of optimal transport problems on an Euclidean space using solutions of optimal

transport problems on graphs. Towards this end, we partition  $M$  into  $m$   $d$ -dimensional connected, positive volume subsets  $P_m = \{B_1, B_2, \dots, B_m\}$ . Additionally, we assume that the boundaries  $\partial B_i$  are piecewise smooth. Then we can consider the optimal transport problem on a graph  $\mathcal{G} = (\mathcal{V}, \mathcal{E})$  where the cardinality of  $\mathcal{V}$  is  $m$  and the connectivity of the graph is determined by the topology of  $M$  and the partition  $P_m$ . More specifically,  $\mathcal{V} = \{1, 2, \dots, m\}$  and an element  $e = (v \rightarrow w) \in \mathcal{E}$  for  $v, w \in \mathcal{G}$  and  $v \neq w$  if  $\bar{B}_v \cap \bar{B}_w$  has non-zero  $d - 1$ -dimensional measure. The graph  $\mathcal{G}$  is *strongly connected*, i.e., for any two vertices,  $v_0, v_T \in \mathcal{V}$  there exists a directed path of  $r$  vertices,  $(v_1, v_2, \dots, v_r)$  in  $\mathcal{V}$ , such that  $(v_i \rightarrow v_{i+1}) \in \mathcal{E}$  for each  $i \in \{1, 2, \dots, r - 1\}$ . Moreover, this graph is also *symmetric*, that is,  $e = (v \rightarrow w) \in \mathcal{E}$  implies  $\bar{e}$  defined by  $\bar{e} = (w \rightarrow v)$  is also in  $\mathcal{E}$ .

In order to apply the approximation procedure highlighted in [59] we express the continuity Eq. (33), as a bilinear control system,

$$\dot{y}(t) = \mathcal{A}_0(t)y + \sum_{i=1}^n \mathcal{A}_i(\hat{u}_i(t)y(t)) \quad (34)$$

where  $\mathcal{A}_0(t) = -\nabla \cdot (g_0(x, t) \cdot)$  for each  $t \in [0, 1]$ ,  $\hat{u}_i(t) = u_i(\cdot, t)$ ,  $y(t) = \rho(\cdot, t)$ ,  $\mathcal{A}_i = -\nabla \cdot (g_i(x) \cdot)$ . Note that the right hand side of a bilinear system is traditionally expressed in the form  $A(t)\rho(t) + u(t)B\rho(t)$  in control theory literature [65]. The form in Eq. (34) is equivalent for systems on finite-dimensional state spaces, but not for general infinite dimensional bilinear systems if  $\hat{u}(t)$  is not a scalar for each  $t \in [t_0, t_f]$ . For example, in the continuity equation, one can see that  $u(x, t)\nabla \cdot (\rho(x, t)) \neq \nabla \cdot (u(x, t)\rho(x, t))$  in general. Hence, the form Eq. (34) is more appropriate for expressing the system in Eq. (33).

In Section 2.3, it was discussed how generators of semigroups corresponding to the continuity equation can be used to define an approximating semigroup on a graph generated by appropriately constructed transition rate matrices. This method can be generalized to the controlled continuity equation, Eq. (33). A natural extension is to consider approximations of the control operators  $\mathcal{A}_i$  using corresponding transition rate matrices, and analogously construct a controlled Markov chain on the space  $\mathcal{V}$ . However, we note that typically for a controlled Markov chain, the control parameters are constrained to be non-negative. Hence, a direct approximation of  $\mathcal{A}_i$  using transition rate matrices and constraining  $\hat{u}_i(t)$  to be positive would negate the possibility that one can flow both backward and forward along the control vector fields, which is critical for controllability of the system. Hence, to account for this in the approximation procedure, we define a bilinear control system equivalent to the one in Eq. (34), but with positivity constraints on the control:

$$\dot{y}(t) = \mathcal{A}_0(t)y + \sum_{s \in \{+, -\}} \sum_{i=1}^n \mathcal{A}_i^s(\hat{u}_i^s(t)y(t)) \quad ; \quad \hat{u}_i^s(t) \geq 0 \quad (35)$$

where  $\mathcal{A}_i^+ = -\mathcal{A}_i^- = \mathcal{A}_i$  for each  $i \in \{1, 2, \dots, N\}$ .

Using the methodology introduced in Section 2.3, for each of the operators  $\mathcal{A}_0, \mathcal{A}_i^s$ , we construct the control operators on the graph  $\mathcal{G}$ , which are denoted by  $A_0 : [0, T] \times \mathcal{E} \rightarrow \mathbb{R}^+$



and  $A_i^s : \mathcal{E} \rightarrow \mathbb{R}^+$  (Recall that only  $g_0$  is possibly time-varying, while  $g_i$ ,  $i > 0$ , are all time-invariant). The difference is that while generators in Section 2.3 were defined as *vertex-based*  $|\mathcal{V}| \times |\mathcal{V}|$  transition rate matrices, here we construct *edge-based* vectors of size  $|\mathcal{E}|$  in a natural way. Hence,  $A_0$  is the edge-based version of the generator constructed from the vector field  $g_0(\mathbf{x}, t)$  using the formula in Eq. (24). For  $A_i^s$ , the corresponding transition rates are defined as

$$A_i^+(e) = A_i^+(v \rightarrow w) = \frac{1}{m(B_w)} \int_{\bar{B}_v \cap \bar{B}_w} \max\{g_i(x) \cdot \mathbf{n}_{vw}, 0\} dm_{d-1}(x), \quad (36)$$

$$A_i^-(e) = A_i^-(v \rightarrow w) = \frac{1}{m(B_w)} \int_{\bar{B}_v \cap \bar{B}_w} \max\{-g_i(x) \cdot \mathbf{n}_{vw}, 0\} dm_{d-1}(x), \quad (37)$$

for  $(i = 1, \dots, n)$  and where  $\mathbf{n}_{vw}$  is the unit normal vector pointing out of  $B_v$  into  $B_w$  at  $x$ .

Let  $\mathcal{P}(\mathcal{V})$  be the space of probability densities on the finite state space,  $\mathcal{V}$ . Then using the above parameter definitions, we consider the following flows on the graph,  $\mathcal{G}$

$$\begin{aligned} \frac{d}{dt} \mu(t, v) = & \sum_{e=(w \rightarrow v)} A_0(t, e) \mu(t, w) - \sum_{e=(v \rightarrow w)} A_0(t, e) \mu(t, v) \\ & + \sum_{s \in \{+, -\}} \sum_{i=1}^n \sum_{e=(w \rightarrow v)} A_i^s(e) U_i^s(t, e) \mu(t, w) - \sum_{s \in \{+, -\}} \sum_{i=1}^n \sum_{e=(v \rightarrow w)} A_i^s(e) U_i^s(t, e) \mu(t, v), \end{aligned} \quad (38)$$

where  $\mu(t, \cdot) \in \mathcal{P}(\mathcal{V})$  for each  $t \in [0, T]$ , and  $U_i^s(t, \cdot)$  are the edge-dependent non-negative ‘control’ parameters that scale the transition rates,  $A_i^s(e)$ . We associate a set of edges  $\mathcal{E}_i^s$  with the above controlled flow. For each  $s \in \{+, -\}$  and  $i \in \{1, 2, \dots, n\}$  we set  $e \in \mathcal{E}_i^s$  if  $A_i^s(e) \neq 0$ . Similarly, we define  $\mathcal{E}_0$  by setting  $e \in \mathcal{E}_0$  if  $A_0(t, e) \neq 0$  for some  $t \in [0, 1]$ . Using these definitions we define the *control graph*  $\mathcal{G}_c = (\mathcal{V}, \mathcal{E}_c)$  by setting  $\mathcal{E}_c = \cup_{s \in \{+, -\}} \cup_{i=1}^n \mathcal{E}_i^s$ , and the *drift graph*  $\mathcal{G}_0 = (\mathcal{V}, \mathcal{E}_0)$ . These definitions will be used in Section 3.2.

The above defined flows can be shown to correspond to the evolution of a time-inhomogeneous continuous-time Markov chain on the finite state space,  $\mathcal{V}$ . The evolution of the corresponding stochastic process  $X(t) \in \mathcal{V}$  over an edge,  $e = (w \rightarrow v) \in \mathcal{E}$ , is defined by the conditional probabilities:

$$\mathbb{P}(X(t+h) = v | X(t) = w) = A_0(t, e) + \sum_{s \in \{+, -\}} \sum_{i=1}^n \sum_{e=(w \rightarrow v)} A_i^s(e) U_i^s(t, e) + o(h). \quad (39)$$

This leads us to the approximating optimal transport problem on a graph, motivated by the formulation in Section 2.4:

$$\tilde{W}(\mu_0, \mu_1) = \inf_{U_i^s(t, e) \geq 0, \mu(t, v) \geq 0} \sum_{s \in \{+, -\}} \sum_{i=1}^n \int_0^1 \|U_i^s(t, \cdot)\|_{\mu(t, \cdot)} dt \quad (40)$$

such that Eq. (38) holds, and

$$\mu(0, v) = \mu_0(v), \mu(1, v) = \mu_1(v) \quad \forall v \in \mathcal{V}$$

The convex formulation of the above problem is then given by

$$\tilde{W}(\mu_0, \mu_1)^2 = \inf_{J_i^s(t,e) \geq 0, \mu(t,v) \geq 0} \sum_{s \in \{+, -\}} \sum_{i=1}^n \int_0^1 \sum_{e=(v \rightarrow w)} \frac{J_i^s(t,e)^2}{2} \left( \frac{1}{\mu(t,v)} + \frac{1}{\mu(t,w)} \right) dt \quad (41)$$

$$\mu(0, v) = \mu_0(v), \mu(1, v) = \mu_1(v) \quad \forall v \in \mathcal{V}$$

$$\frac{d}{dt} \mu(t, \cdot) = \sum_{e=(w \rightarrow v)} A_0(t, e) \mu(t, w) - \sum_{e=(v \rightarrow w)} A_0(t, e) \mu(t, v) + \sum_{s \in \{+, -\}} \sum_{i=1}^n (D_i^s)^\top J_i^s(t, \cdot), \quad (42)$$

where  $J_i^s(t, e) \triangleq \mu(t, v) U_i^s(t, e)$  for  $e = (v \rightarrow w)$ ,  $i = \{1, 2, \dots, n\}$ , and  $D_i^s \in \mathbb{R}^{|\mathcal{E}_i^s| \times |\mathcal{V}|}$  is the linear flow operator computing  $\mu(w) - \mu(v)$  for each  $e = (v \rightarrow w) \in \mathcal{E}_i^s$ .

*Remark 3.1.* We note that the controlled advection equation Eq. (38), and the corresponding convex optimal transport problem in Eq. (41) can be simplified if control vector fields are uni-directional across all boundaries  $\partial B_i$ . This can often be achieved by choosing the grid carefully, and making the subvolumes  $B_i$  small enough. If this condition holds, then we immediately see from Eqs. (36-37) that for each edge  $e = (v \rightarrow w)$ , only one of  $A_i^+(e)$  and  $A_i^-(e)$  is non-zero. Denote the non-zero matrix by  $A_i(e)$ . It also follows that  $A_i(e) = A_i(\bar{e})$ , where  $\bar{e} = (w \rightarrow v)$ . Then the simplified version of Eq. (38) is

$$\begin{aligned} \frac{d}{dt} \mu(t, v) &= \sum_{e=(w \rightarrow v)} A_0(t, e) \mu(t, w) - \sum_{e=(v \rightarrow w)} A_0(t, e) \mu(t, v) \\ &+ \sum_{i=1}^n \sum_{e=(w \rightarrow v)} A_i(e) U_i(t, e) \mu(t, w) - \sum_{i=1}^n \sum_{e=(v \rightarrow w)} A_i(e) U_i(t, e) \mu(t, v). \end{aligned} \quad (43)$$

This results in the following convex optimal transport problem,

$$\tilde{W}(\mu_0, \mu_1)^2 = \inf_{J_i(t,e) \geq 0, \mu(t,v) \geq 0} \sum_{i=1}^n \int_0^1 \sum_{e=(v \rightarrow w)} \frac{J_i(t,e)^2}{2} \left( \frac{1}{\mu(t,v)} + \frac{1}{\mu(t,w)} \right) dt, \quad (44)$$

$$\mu(0, v) = \mu_0(v), \mu(1, v) = \mu_1(v), \quad \forall v \in \mathcal{V}$$

$$\frac{d}{dt} \mu(t, \cdot) = \sum_{e=(w \rightarrow v)} A_0(t, e) \mu(t, w) - \sum_{e=(v \rightarrow w)} A_0(t, e) \mu(t, v) + \sum_{i=1}^n (D_i)^\top J_i(t, \cdot). \quad (45)$$

*Remark 3.2.* We note that the Eq. (25) discussed in Section 2.4 can be seen as the special case of Eq. (43) with  $g_0 \equiv 0$  and  $g_i = \hat{i}$  (the  $i$ th unit vector). Hence, our formulation generalizes optimal transport on graphs from a single-integrator system to general nonlinear control-affine systems. While a rigorous proof of convergence of  $\tilde{W}$  as defined in Eq. (40) or Eq. (44) to  $W_2$  is not provided here, the connection to Eq. (25) provides a heuristic argument in this direction. As discussed in Section 2.4, Ref. [62] provides such a convergence proof for an advection equation on graphs. The advection is modeled using anti-symmetric discrete

‘momentum vector fields’  $V$  on the edges, and the optimal transport problem minimizes a discrete action. For the driftless case, Eq. (43) satisfies those conditions due to the way the transition matrices  $A_i(e)$  (which give edge-weights) are defined, and our definition of  $\tilde{W}$  agrees with the one given in Ref. [62]. We also note in general when  $A_0 \neq 0$ , the solution of the optimization problem  $\tilde{W}$  does not necessarily define a metric on  $\mathcal{P}(\mathcal{V})$  due to the asymmetry that is possibly induced by the drift vector fields.

### 3.2 Controllability Analysis of Flow over Graphs

In this section, we establish that the controlled Markov chain approximations Eq. (38) preserve the controllability properties of the system in Eq. (31). This will ensure the well-posedness of the graph optimal transport problem, Eq. (40). Without loss of generality, we consider the case when  $t_0 = 0$  &  $t_f = 1$ . First, we recall a few standard notions from geometric control theory [66].

*Definition 3.3.* Given  $x_0 \in M$  we define  $R(x_0, t)$  to be the set of all  $x \in M$  for which there exists an admissible control  $\mathbf{u} = (u_1, u_2, \dots, u_n)$  such that there exists a trajectory of system in Eq. (31) with  $x(0) = x_0$ ,  $x(t) = x$ . The **reachable set from  $x_0$  at time  $T$**  is defined to be

$$R_T(x_0) = \cup_{0 \leq t \leq T} R(x_0, t) \quad (46)$$

*Definition 3.4.* We say the system in Eq. (31) is **small-time locally controllable** from  $x_0$  if  $x_0$  is an interior point of  $R_T(x_0)$  for any  $T > 0$ .

*Definition 3.5.* Let  $f = (f_1, \dots, f_d)$  and  $g = (g_1, \dots, g_d)$  be two smooth vector fields on  $\cdot$ . Then the **Lie bracket**  $[f, g]$  is defined to be the vector field with components

$$[f, g]^i = \sum_{j=1}^n \left( f^j \frac{\partial g^i}{\partial x^j} - g^j \frac{\partial f^i}{\partial x^j} \right) \quad (47)$$

*Definition 3.6.* For a collection of vector fields  $\{g_i\}$ , **Lie** $\{g_i\}$  refers to the smallest Lie sub-algebra of set of smooth vector fields on  $M$  that contains  $\{g_i\}$ . **Lie<sub>x</sub>** $\{g_i\}$  refers to the span of all vector fields in **Lie** $\{g_i\}$  at  $x \in M$

We will use the notation  $\text{int}(S)$  to refer to the interior of a set  $S$ . Using these definitions we have the following result

*Theorem 3.7.* Suppose one of the following statements is true:

1.  $g_0 \equiv 0$  and  $\text{Lie}_x \left\{ g_i : i \in \{1, 2, \dots, n\} \right\} = T_x M$  at each  $x \in \text{int}(M)$ .
2.  $\text{span} \left\{ g_i(x) : i \in \{1, 2, \dots, n\} \right\} = T_x M$  at each  $x \in \text{int}(M)$ .

Then the graph  $\mathcal{G}_c$  associated with the system in Eq. (38) is strongly connected and  $\mathcal{G}_c = \mathcal{G}$ .

*Proof.* Let  $v, w \in \{1, 2, \dots, N\}$  be such that  $v \neq w$  and  $\bar{B}_v \cap \bar{B}_w$  has non-zero  $(d-1)$ -dimensional (Hausdorff) measure. Consider points  $x_0 \in \text{int}(B_v)$  and  $x_1 \in \text{int}(B_w)$ . Due to connectedness of  $M$  there exists a continuous path  $\gamma : [0, 1] \rightarrow M$  such that  $\gamma(0) = x_0$ ,  $\gamma(1) = x_1$  and  $\gamma(t) \in B_v \cup B_w \forall t \in [0, 1]$ . From the Lie bracket condition of the vector fields, it follows that the system is small-time locally controllable at every  $x \in \text{int}(M)$ . Hence, we can approximate the path  $\gamma$  using a trajectory of the control system, using a sequence of piecewise-constant control inputs. Particularly, for each  $\epsilon > 0$  there exists  $k \in \mathbb{N}$  large enough, a time sequence  $t_1, t_2, \dots, t_k$  satisfying  $\sum_{i=1}^k t_i = 1$ , constant control inputs  $u^1, u^2, \dots, u^k \in \mathbb{R}$  and an approximating path,  $f : [0, 1] \rightarrow M$  defined as

$$f\left(\sum_{i=1}^j t_i + \tau\right) = e^{t_1 u^1 h_1} \circ \dots \circ e^{t_j u^j h_j} \circ e^{\tau u^{j+1} h_{j+1}} x_0 \quad \text{for each } j \in \{0, 1, \dots, m\} \text{ and } \tau \in [0, t_{j+1}], \quad (48)$$

such that  $\|\gamma(s) - f(s)\|_2^2 \leq \epsilon$  for all  $s \in [0, 1]$ . Here, the case  $j = 0$  means  $f(\tau) = e^{\tau u^1 h_1} x_0$  for all  $\tau \in [0, t_1]$ . Let  $s \in (0, 1)$  be such that  $f(s) \in \partial B_v$  and there exists  $c \in (0, s)$  small enough such that  $f(s-c) \in \text{int}(B_v)$  and  $f(s+c) \in \text{int}(B_w)$ . Then, clearly  $\mathbf{n}_{vw} \cdot g_r(x) \neq 0$  for some  $r \in \{1, 2, \dots, n\}$  and some  $x$  in an open neighborhood of  $f(s)$  that is completely contained in  $B_v \cup B_w$ , assuming  $\gamma$  and  $\epsilon$  are chosen appropriately (i.e. avoiding crossings of  $\gamma$  and  $f$  over corners of  $B_v$  and  $B_w$ ). If not,  $f(s+\delta) \in \partial B_i$  for all  $\delta \in (0, c]$  since the non-existence of such a point in the neighborhood of  $f(s)$  implies one cannot use a concatenation of flows associated with the control vector fields to leave the set  $\partial B_v$ , which leads to a contradiction. From continuity of the vector field  $g_r$ , there exists a small enough neighborhood,  $N_x$  of  $x$  such that  $\mathbf{n}_{vw} \cdot g_r(y) \neq 0$  for all  $y \in N_x$ . Hence, this implies  $A_r^s(e) \neq 0$  for  $e = v \rightarrow w$  for some  $s \in \{+, -\}$ . Due to continuity of the vector field  $g_r$  at  $x$ , it also follows that  $A_r^s(e) = A_r^s(\bar{e})$ . Hence, the connectivity of the graph  $\mathcal{G}_c$  follows. Case 2 just follows from the assumption that  $\text{span}\left\{g_i(x) : i \in \{1, 2, \dots, n\}\right\} = T_x M$  at each  $x \in \text{int}(M)$ .  $\square$

*Remark 3.8.* The above result can also be seen to, equivalently, follow from the Orbit theorem [67][Theorem 5.1].  $\mathcal{G}_c \neq \mathcal{G}$  would imply the existence of a lower dimensional *immersed-submanifold*,  $K$ , of  $M$  such that  $\text{Lie}_x\left\{g_i : i \in \{1, 2, \dots, n\}\right\} \subseteq T_x K$  for all  $x$  in a neighborhood of a point in the boundary of one of the elements in  $P_m$ .

*Remark 3.9.* The main obstruction in extending the above result for underactuated systems ( $\text{span}\left\{g_i(x) : i \in \{1, 2, \dots, n\}\right\} \neq T_x M$  for some  $x \in M$ ) with drift, i.e.  $g_0 \neq 0$ , is that usual tests for small-time local controllability of control systems with drift [68] require the initial condition to be an equilibrium point. Hence, starting at a non-equilibrium initial condition one might need to make large excursions (in our case, possibly outside the domain  $M$ ) in order to return to the initial condition. Take for example, the simplest control-affine system with drift, the double integrator:  $\ddot{x} = u$ . Hence, given an initial and target density, the

optimal transport problem on a bounded domain might not admit a solution for a system with drift if  $M$  is not taken to be large enough.

We note the following result to ensure well-posedness of problem given in Eq. (40). The proof follows from a more general result proved in Ref. [69] where the controllability result was proved for the case when  $A_i(t, e)$  is either equal to 0 or 1 for each  $i \in \{1, 2, \dots, n\}$  and each  $e \in \mathcal{G}_c$  and  $\mathcal{G}_c$  is only required to be strongly connected. Here we give an alternative proof for the case when  $\mathcal{G}_c$  is strongly connected and symmetric, to keep the paper self-contained.

*Theorem 3.10. Consider  $\mu_0, \mu_1 \in \text{int}(\mathcal{P}(\mathcal{V}))$  where  $\text{int}(\mathcal{P}(\mathcal{V})) = \{\mu \in \mathcal{P}(\mathcal{V}); \mu(v) > 0 \text{ for each } v \in \mathcal{V}\}$  is the interior of the set  $\mathcal{P}(\mathcal{V})$  and  $A_0(t, e) = 0$  for every  $e \in \mathcal{E}$  and all  $t \in [0, 1]$ . Then there exist piecewise continuous  $U_i^s(t, \cdot) \geq 0$  such that the solution of Eq. (38),  $\mu(t, \cdot)$  satisfies  $\mu(0, \cdot) = \mu_0$  and  $\mu(1, \cdot) = \mu_1$ .*

*Proof.* We can represent the equation (38) as a bilinear control system of the form

$$\frac{d}{dt}\mu(t, \cdot) = \sum_{s \in \{+, -\}} \sum_{i=1}^n \sum_{e=(v \rightarrow w)} A_i^s(e) U_i^s(t, e) B_e^{si} \mu(t, \cdot) \quad (49)$$

where  $B_e^{si} \in \mathbb{R}^{m \times m}$  is given by

$$(B_e^{si})_{pq} = \begin{cases} -1 & \text{if } p = q = v \\ 1 & \text{if } p = w, q = v \\ 0 & \text{otherwise} \end{cases}$$

for each  $s \in \{+, -\}$ ,  $i \in \{1, 2, \dots, n\}$  and  $e = (v \rightarrow w) \in \mathcal{E}$ . Here,  $(B_e^{si})_{pq}$  denotes the element in the  $p^{\text{th}}$  row and  $q^{\text{th}}$  column of the matrix  $B_e^{si}$ . Corresponding to the graph,  $\mathcal{G}_c$ , we define the adjacency matrix  $A_c$  defined by

$$(A_c)_{pq} = \begin{cases} 1 & \text{if } (p \rightarrow q) \in \mathcal{E}_c \\ 0 & \text{otherwise} \end{cases}$$

Additionally, the degree matrix is a diagonal matrix  $D_c$  where the diagonal elements  $(D_c)_{jj}$  are equal to the total number of edges leaving the node  $j \in \mathcal{V}$ . Then the Laplacian matrix  $L_c$  associated with the graph  $\mathcal{G}_c$  is given by  $L_c = A_c - D_c$ . Since, the graph is symmetric  $L_c$  is a symmetric matrix. Alternatively, the Laplacian  $L_c$  of the graph  $\mathcal{G}_c$  can also be expressed as  $L_c = \sum_{s \in \{+, -\}} \sum_{i=1}^n \sum_{e \in \mathcal{E}_{sub}^{si}} B_{ie}^s$  for some subsets  $\mathcal{E}_{sub}^{si}$  of the set of edges  $\mathcal{E}_c$  such that  $A_i^s(e) \neq 0$  for each  $s \in \{+, -\}$  and  $i \in \{1, 2, \dots, n\}$  such that  $e \in \mathcal{E}_{sub}^{si}$ . Since,  $\mathcal{G}_c$  is strongly connected and symmetric it follows that the rank of the matrix  $L_c$  is  $m - 1$ . Let  $\mathbf{1}$  and  $\mathbf{0}$  be vectors of dimension  $m$  with all elements equal to 1 and 0 respectively. Then we know that that  $(B_e^{si} \mathbf{1})^T \mathbf{1} = 0$  for each  $s \in \{+, -\}$  and  $i \in \{1, 2, \dots, n\}$  such that  $e \in \mathcal{E}_{sub}^{si}$ . This implies that span of the set  $\mathcal{B} = \cup_{s \in \{+, -\}} \cup_{i=1}^n \cup_{e \in \mathcal{E}_{sub}^{si}} \{B_{ie}^s \mathbf{1}\}$  is equal to the tangent space

$T_x(\mathcal{P}(\mathcal{V}))$  of  $\mathcal{P}(\mathcal{V})$  at every  $x \in \text{int}(\mathcal{P}(\mathcal{V}))$ . Here, we are identifying the set  $T_x(\mathcal{P}(\mathcal{V}))$  with the set  $\{y \in \mathbb{R}^m; \sum_{j=1}^m y_j = 0\}$ . Let  $\tilde{\mathcal{E}}_{sub}^{si}$  be subsets of  $\mathcal{E}_{sub}^{si}$ , such that the elements of  $\tilde{\mathcal{B}} = \cup_{s \in \{+, -\}} \cup_{i=1}^n \cup_{e \in \tilde{\mathcal{E}}_{sub}^{si}} \{B_{ie}^s \mathbf{1}\}$  are linearly independent and span the set  $T_x(\mathcal{P}(\mathcal{V}))$  at every  $x \in \text{int}(\mathcal{P}(\mathcal{V}))$ .

Next, we note that  $\text{int}(\mathcal{P}(\mathcal{V}))$  is convex and hence there exists an atleast-once-differentiable path  $\gamma : [0, T] \rightarrow \text{int}(\mathcal{P}(\mathcal{V}))$  such that  $\gamma(0) = \mu_0$  and  $\gamma(1) = \mu_1$ . Since span of  $\tilde{\mathcal{B}}$  is equal  $T_x(\mathcal{P}(\mathcal{V}))$  at every  $x \in \text{int}(\mathcal{P}(\mathcal{V}))$  and  $\frac{d}{dt}\gamma(t) \in T_{\gamma(t)}(\mathcal{P}(\mathcal{V}))$  at every  $t \in [0, 1]$  it follows that there exist parameters  $\tilde{U}_i^s(t, e)$  that are continuous with respect to time satisfying

$$\frac{d}{dt}\gamma(t) = \sum_{s \in \{+, -\}} \sum_{i=1}^n \sum_{e \in \tilde{\mathcal{E}}_{sub}^{si}} \tilde{U}_i^s(t, e) B_e^{si} \mathbf{1} \quad (50)$$

for all  $t \in [0, 1]$ . Next, for each  $s \in \{+, -\}$  and each  $i \in \{1, 2, \dots, n\}$  we set

$$U_i^s(t, e) = \begin{cases} \frac{\tilde{U}_i^s(t, e)}{A_i^s(e)\mu(t, v)} & \text{if } U_i^s(t, e) \geq 0 \\ 0 & \text{otherwise} \end{cases}$$

and

$$U_i^s(t, \bar{e}) = \begin{cases} -\frac{\tilde{U}_i^s(t, e)}{A_i^s(\bar{e})\mu(t, w)} & \text{if } U_i^s(t, e) \leq 0 \\ 0 & \text{otherwise} \end{cases}$$

whenever  $e \in \tilde{\mathcal{E}}_{sub}^{si}$ , for each  $t \in [0, 1]$ . Additionally, if for a given  $s \in \{+, -\}$  and  $i \in \{1, 2, \dots, n\}$  we have an edge  $e \in \mathcal{E}$  such that  $e \in \mathcal{E}_c \setminus \tilde{\mathcal{E}}_{sub}^{si}$ , then we set

$$U_i^s(t, e) = 0 \quad (51)$$

and

$$U_i^s(t, \bar{e}) = 0 \quad (52)$$

for each  $t \in [0, 1]$ . Note that that  $B_e^{si}\mu(t, \cdot) = \mu(t, v)B_e^{si}\mathbf{1}$  when  $e = (v \rightarrow w)$ . From this, the result follows by noting that for the choice of parameters  $U_i^s(t, e)$  the solution of (38), given by  $\mu(t, \cdot) = \gamma(t)$  for all  $t \in [0, 1]$ .  $\square$

The above proof can also be extended to the case when  $\mathcal{G}_c$  is only strongly connected and not necessarily symmetric. Note that for the case when either of  $(\mu_0, \mu_1)$  lie on the boundary of  $\mathcal{P}(\mathcal{V})$ , controllability of the system in Eq. (38) might not hold, as pointed out in Ref. [69]. This does not affect our numerical results however, and we are able to achieve convergence in all cases we discuss in Section 4.

Theorem 3.10 leads to the following result:

*Theorem 3.11. Consider  $\mu_0, \mu_1 \in \text{int}(\mathcal{P}(\mathcal{V}))$ . Assume the graph  $\mathcal{G}_c$  is connected and  $\mathcal{G}_0 \subseteq \mathcal{G}_c$ . Then there exist  $U_i(t, \cdot) \geq 0$  such that Eq. (38) satisfies  $\mu(0, \cdot) = \mu_0$  and  $\mu(1, \cdot) = \mu_1$ .*

*Proof.* The graph  $\mathcal{G}_c$  is connected. Since  $\mathcal{G}_0 \subseteq \mathcal{G}$ , we can choose  $\tilde{U}_i^s(t, \cdot)$  such that the right hand side in Eq. (38) is equal to 0 for all  $t \in [0, 1]$ . Then, from the previous theorem, it follows that there exists a control  $U_i^s(t, \cdot)$ , of the form  $U_i^s(t, \cdot) = \hat{U}_i^s(t, \cdot) + \tilde{U}_i^s(t, \cdot)$  such that Eq. (38) satisfies  $\mu(0, \cdot) = \mu_0$  and  $\mu(1, \cdot) = \mu_1$ . Here, the parameter  $\tilde{U}_i(t, \cdot)$  negates the effect of the drift field  $A_0$  and  $\hat{U}_i^s(t, \cdot)$  ensures the density  $\mu_0$  is transported to  $\mu_1$  as in Thm 3.10.  $\square$

### 3.3 Construction of Approximate Feedback Control Laws

Given the solution the optimal transport problem on the graph, we need to reconstruct the corresponding approximate feedback control laws  $\{u_i(x, t)\}$ . The feedback control laws for the control system in Eq. (31) are given by

$$u_i(x, t) = \frac{\sum_{w \in \mathcal{N}_i^+(v)} U_i^+(v \rightarrow w, t)}{|\mathcal{N}_i^+(v)|} - \frac{\sum_{w \in \mathcal{N}_i^-(v)} U_i^-(v \rightarrow w, t)}{|\mathcal{N}_i^-(v)|} \quad \forall x \in B_v \quad (53)$$

Here,  $\mathcal{N}_i^s(v)$  refers to the the neighboring nodes of  $v$  in the graph  $(\mathcal{V}, \mathcal{E}_i^s)$  for each  $s \in \{+, -\}$  and  $i \in \{1, 2, \dots, n\}$ .

### 3.4 Numerical Implementation

We adapt the numerical scheme used in Refs. [70, 64] to our setting, and use a staggered discretization scheme for pseudo-time discretization. We define

$$\mu_j(v) \triangleq \mu(t_j, v), \quad (54)$$

$$J_{i,j}^s(e) \triangleq J_i^s(t_j, e), \quad (55)$$

where  $t_j = (j/k)t_f, j \in [0, 1, 2, \dots, k]$  is the time discretization into  $k$  intervals. We take  $t_0 = 0$ . Here  $J_{i,j}^s(e)$  represents the  $s \in \{+, -\}$  flow due to  $g_i(x)$  over edge  $e = (v \rightarrow w)$ , from vertex  $v$  at time  $t_j$  to vertex  $w$  at time  $t_{j+1}$ .

Hence, the optimization problem given in Eqs. (41) can discretized as,

$$\tilde{W}(\mu_0, \mu_1)^2 = \inf_{J_{i,j}^s \geq 0, \mu_j \geq 0} \sum_{s \in \{+, -\}} \sum_{i=1}^n \sum_{j=1}^k \sum_{\substack{e=1 \\ e=(v \rightarrow w)}}^{|\mathcal{E}_i^s|} (J_{i,j}^s(e))^2 \left( \frac{1}{\mu_j(v)} + \frac{1}{\mu_{j+1}(w)} \right), \quad (56)$$

subject to the following constraints:

$$\frac{\mu_{j+1} - \mu_j}{\Delta t} = A_0(t_j)\mu_j + \sum_{s \in \{+, -\}} \sum_{i=1}^n (D_i^s)^\top J_s^{i,j}, \quad (57)$$

$$\mu_0 = \mu_{t_0}, \mu_k = \mu_{t_f}, \quad (58)$$

where we have used the vertex-based  $m \times m$  transition rate matrix  $A_0(t_j)$  as originally defined in Eq. (24). Here  $\Delta t = \frac{t_f}{k}$ . The cost function given by Eq. (56) is again of the form ‘quadratic over linear’, and the advection (Eq. (57)) imposes linear constraints. Hence the discretized problem is convex, and can be solved using many off-the-shelf convex solvers. The optimization problem is solved via CVX [71] modeling platform, an open-source software for converting convex optimization problems into usable format for various solvers. We use the SCS [72] solver, a first-order solver for large size convex optimization problems. This solver uses the Alternating Direction Method of Multipliers (ADMM) [73] to enable quick solution of very large convex optimization problems, with moderate accuracy.

The variables to be solved for in the optimization problem Eqs. (56-58) are vertex based quantities  $\mu_j$ , and edge based quantities  $J_{i,j}^s$ . The size of the optimization problem can be quantified in terms of number of time-discretization steps  $k$ , number of vertices  $|\mathcal{V}| = m$ , and the number of edges  $|\mathcal{E}_c|$ . The graph  $\mathcal{G}_c$  is always sparse, since a typical vertex is at most connected to  $2(n+1)d$  neighbors, and  $m \gg n, m \gg d$ . Hence, the variables in the optimization problem scale as  $O(k(m + |\mathcal{E}|)) = O(n \cdot d \cdot k \cdot m)$ .

## 4 Examples

### 4.1 Optimal Transport in the Grushin Plane

We first apply our framework to a non-holonomic control-affine system in which certain optimal transport solutions can be found analytically. We consider transport of measure in the Grushin plane, which is a subriemannian space, with base space  $\mathbb{R}^2$ . In Ref. [54], the structure of optimal controls in this problem was analyzed. Using this structure, optimal transport to a delta measure at  $(0,0)$  was computed. The system is described by

$$\dot{x}_1 = u_1, \tag{59a}$$

$$\dot{x}_2 = u_2 x_1. \tag{59b}$$

The optimal control cost  $c(x, y)$  between initial and final states,  $x = (x_1, x_2)^\top, y = (y_1, y_2)^\top$ , is taken to be square of the subriemannian distance  $d(x, y) = \inf_{u_x^y} \int_0^1 \sqrt{u_1^2 + u_2^2} dt$ . Hence, the optimal control solutions are also geodesics in the subriemannian space. The solutions of optimal control problem are integral curves of the Hamiltonian  $H$  given by

$$H(x_1, x_2, p_1, p_2) = \frac{1}{2}(p_1^2 + x_1^2 p_2^2). \tag{60}$$

Here  $p_1, p_2$  are the co-state variables. Note that since  $H$  is independent of  $x_2$ ,  $H$  can be reduced to a Hamiltonian in  $(x_1, p_1)$ , and the integral curves of  $H$  can be obtained using quadratures. The geodesics reaching  $(0, \alpha)$  at  $t = 1$  are of the form

$$x_1(t) = \frac{a}{b} \sin(b(1-t)), \tag{61}$$

$$x_2(t) = \frac{a^2}{4b^2} (2b(1-t) - \sin(2b(1-t))) + \alpha. \tag{62}$$



A geodesic between a specified initial point  $(\bar{x}_1, \bar{x}_2)$ , and  $(0, \alpha)$  can be obtained by inverting the Eqs. (61-62) at  $t = 0$  to solve for  $(a, b)$ . For  $t \leq \frac{\pi}{b}$ , these geodesics are also global minimizers of the optimal control problem. Figure 2(a) shows some geodesics to the origin. Now consider the optimal transport problem with  $c(x, y) = d^2$  from an initial measure  $\mu_0$  to final measure  $\mu_1 = \delta_{(0,0)}$ . Clearly, the optimal map  $T$  is  $x \rightarrow (0, 0)$ , and the displacement interpolation is given by the geodesics between each  $x \in \text{supp}(\mu_0)$  and  $(0, 0)$ . Figure 2(b) shows the displacement interpolation of  $T$  for a particular case.

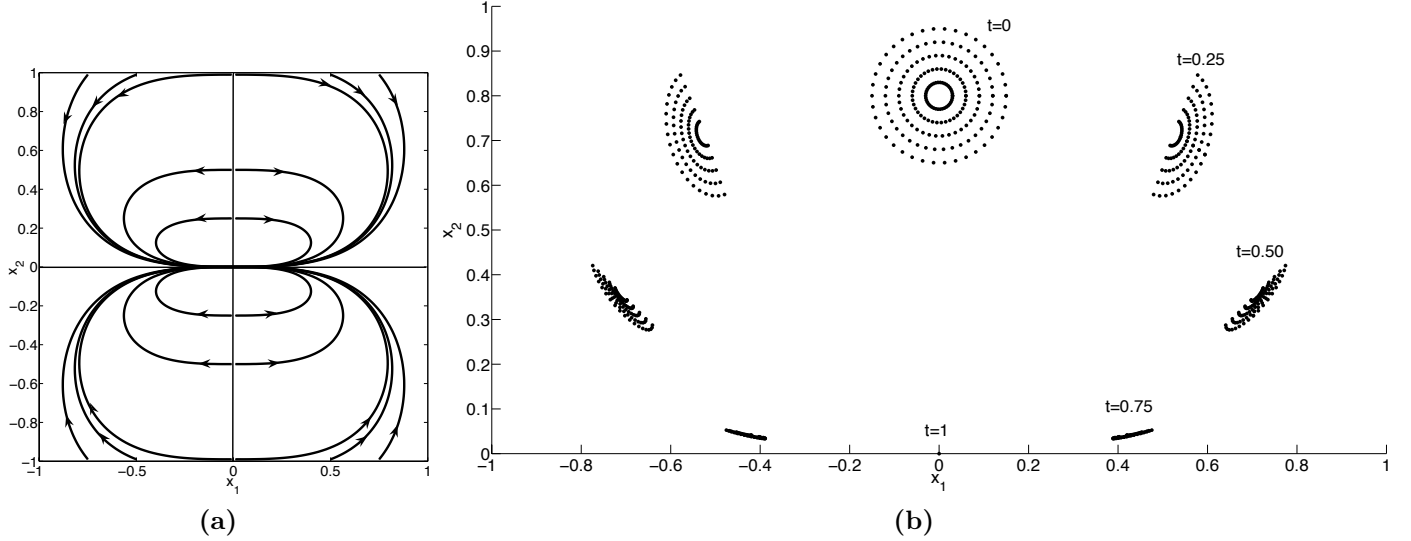


**Figure 2:** (a) Some minimizing geodesics to the origin in the Grushin plane. (b) Analytically computed optimal transport solution between a measure whose support is the disk  $\Omega = \{(x, y) | x^2 + (y - .8)^2 < .15^2\}$ , and measure at the box containing the origin.

We apply the our computational framework algorithm developed in Section 3 to compute optimal transport for a similar case as described above. We divide the  $X = [-1, 1] \times [-1, 1]$  into  $m = 100^2$  boxes, and form the corresponding graph  $\mathcal{G}$ . The resulting solution is shown in Figure 3(a)-(e). The convergence of optimal transport cost  $\tilde{W}$  with  $k$  and  $m$  is shown in Fig 3(f). It can be seen that the computed solution closely follows the analytical solution shown in Fig. 2.

Next, we perform particle simulations with feedback controls extracted from the optimal transport computation, using Eq. (53). We take  $p = 4$  particles per box, and use Eq. (53) to get state-dependent control commands for each particle. The results are shown in Figure 4. About 95% of the particles get transported according the optimal transport solution shown in Fig 3, while the rest are dispersed. Note that the control laws obtained from optimal transport solution do not automatically guarantee feedback stabilization of individual particles.

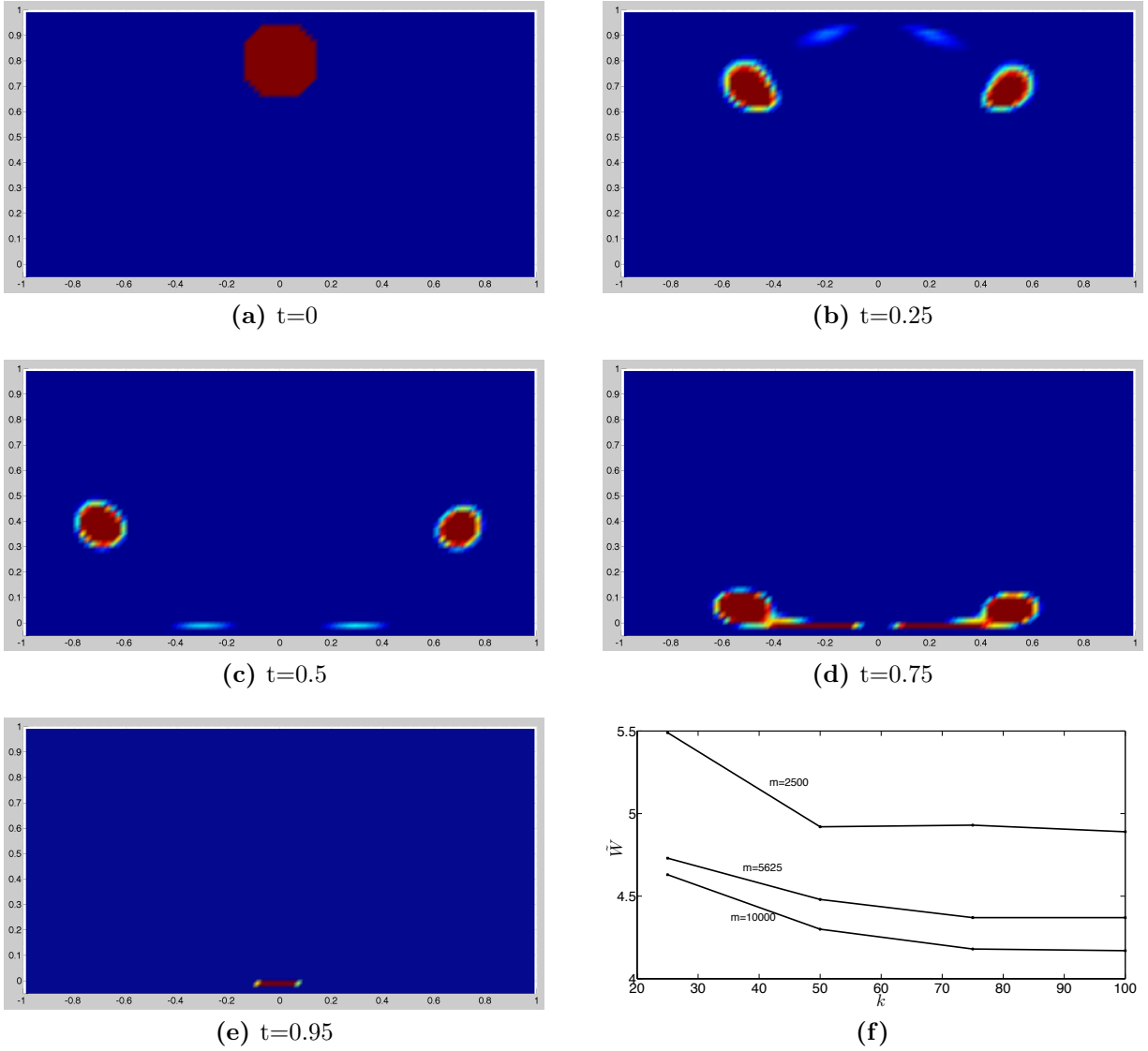


**Figure 3:** (a)-(e) The optimal transport solution in the Grushin plane using graph based algorithm between a measure whose support is the disk  $\Omega = \{(x, y) | x^2 + (y - .8)^2 < .15^2\}$ , and delta measure at the origin. The parameters are  $m = 10^4, k = 75$ . (f) Convergence of optimal transport cost with number of time discretization steps  $k$  and grid size  $m$ .

## 4.2 Optimal Transport in Time-Periodic Double-Gyre system

Now we consider a measure transport problem for the time-periodic double-gyre system [74]. This chaotic dynamical system has been analyzed using several computational tools related to transport and mixing [75, 76, 23, 24, 43].

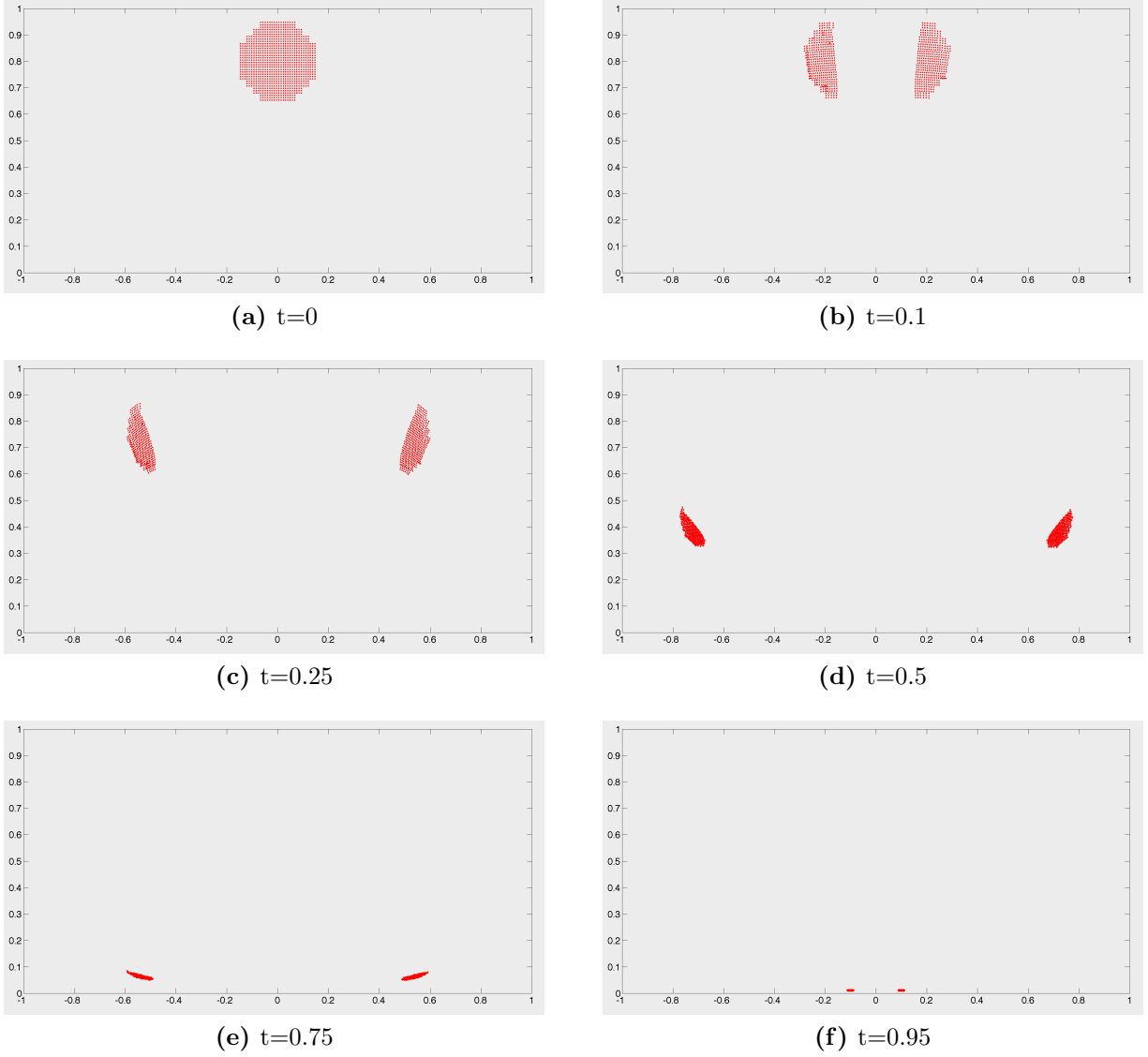


**Figure 4:** Particle trajectories with control computed from the optimal transport solution in the Grushin plane. Each box contained in the support of uniform initial measure  $\mu_0$  is initially populated with 4 particles.

The controlled equations we consider as follows,

$$\dot{x} = -\pi A \sin(\pi f(x, t)) \cos(\pi y) + u_1, \quad (63a)$$

$$\dot{y} = \pi A \cos(\pi f(x, t)) \sin(\pi y) \frac{df(x, t)}{dx} + u_2, \quad (63b)$$

where  $f(x, t) = \beta \sin(\omega t)x^2 + (1 - 2\beta \sin(\omega t))x$  is the time-periodic forcing in the system. The phase space is  $X = [0, 2] \times [0, 1]$ . We first describe the dynamics of the uncontrolled ( $u_1 = u_2 = 0$ ) system. For the trivial case of  $\beta = 0$  (i.e. no time-dependent forcing), the phase space is divided into two invariant sets, i.e., the left and right halves of the rectangular phase

space ('gyres'), by a heteroclinic connection between fixed points  $x_1 = (1, 1)$  and  $x_2 = (0, 1)$ . For non-zero  $\beta$ , the Poincare map  $F$  of the system, obtained by integrating the dynamics over one time period  $\tau$  of  $f$ , describes an autonomous discrete-time system. The heteroclinic connection is broken in this case, and results in a heteroclinic tangle. This heteroclinic tangle leads to transport between left and right sides via lobe-dynamics.

We choose parameters  $A = 0.25, \beta = 0.25, \omega = 2\pi$ , such that the time-period of the flow is  $\tau = 1$ . To get insight into the phase space transport due to heteroclinic tangles, the theory of lobe dynamics [74] is useful. Lobe dynamics techniques allows one to quantify the transport between sets separated by invariant manifolds, and their transversal intersections. In figure 5, the unstable manifold of  $x_1 \approx (0.919, 1)$ ,  $U_{x_1}$ , and the stable manifold of  $x_2 \approx (1.081, 0)$ ,  $S_{x_2}$  are shown in green and white respectively. The lobe labeled 'A', its pre-image  $F^{-1}(A)$  and image  $F(A)$  are also shown. Consider the segment  $L = U_{x_1}(x_1 \rightarrow F(P_1)) \cup S_{x_2}(F(P_1) \rightarrow x_2)$ . Then  $L$  divides phase space  $X$  into two regions. The points that get mapped from left to right region in one iteration of  $F$  are precisely those in set  $A$ . Hence, the amount of mass transport from left to right side of  $L$  is  $\bar{m}(A)$ . While our algorithm for optimal transport

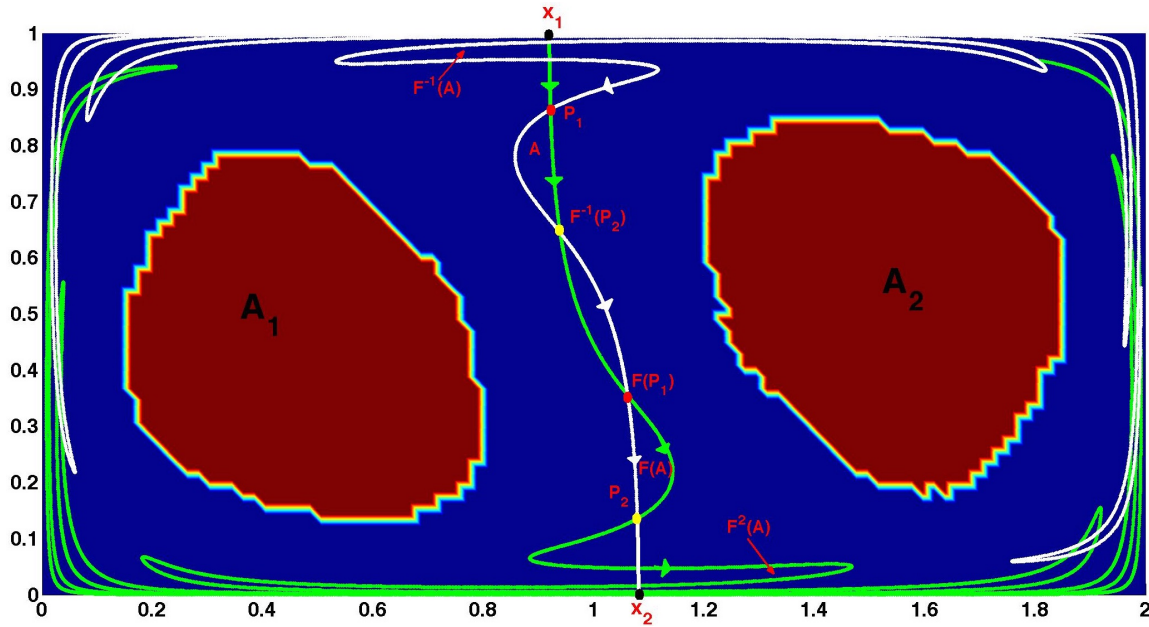


**Figure 5:** Invariant manifolds and lobe-dynamics in the double-gyre system.

can be applied between any arbitrary pair of measures, it is instructive to choose a pair of measures which are somehow ‘distinguished’ for the given system. Selecting a pair of invariant measures is an obvious choice, however the chaotic double-gyre system does not seem to possess any invariant measures except the uniform measure. However, there do exist almost-invariant sets (and associated measures with support on those sets). A set  $S$  is called almost-invariant [23] if

$$\frac{\bar{m}(F^{-1}(S) \cap S)}{\bar{m}(S)} \approx 1.$$

Invariant and almost-invariant sets in this system can be identified by the sign structure of the second eigenvector of the reversibilized transfer operator

$$R = \frac{P + \tilde{P}}{2},$$

where  $P$  is the transfer operator corresponding to  $F$  and  $\tilde{P}$  is the transfer operator for the reverse-time dynamics. In Figure 5, two almost-invariant sets,  $A_1$  and  $A_2$  are also shown. We choose our initial and final measures to be uniform measures supported on  $A_1$  and  $A_2$ , respectively. Both measures are normalized to sum to unity. We solve the optimal transport problem for  $m = 60 \times 30$  for different time horizons  $t_f$ , with  $k = 40$ . Our simulations are repeated with finer grid-sizes  $m = 100 \times 50$  to verify that our results are nearly independent of  $m$ .

In Fig. 6, we show the optimal transport sequence for  $t_f = \tau = 1$ . In other words, the transport is constrained to be completed in one time-period of the uncontrolled flow. Due to the short time-horizon, all of the mass is pushed across the invariant manifolds separating the two gyres. In Fig. 7, the optimal transport sequence for the more interesting case with  $t_f = 10$  is shown. The transport process in this case is completely different than the  $t_f = 1$  case. We observe that the transport occurs in a ‘quantized’ manner, i.e. packets of mass are transported, one at a time, via lobe-dynamics from left gyre to the right gyre. The number of such packets *exactly* equal the number of time-periods in the time-horizon of the transport problem, i.e. 10 in this case. Hence, while the global transport is being done by the natural dynamics via lobes, the role of control is to gather the mass in pre-images of the those lobes. For instance, in Figs 7((b)-(e)), the transport of one such packet via the sequence  $F^{-1}(A) \rightarrow A \rightarrow F(A) \rightarrow F^2(A)$  is shown. The mechanism is essentially the same for other time-horizons that we analyzed,  $t_f = 2, 5, 8, 12.5$  & 15. The increasing use of ‘natural’ chaotic lobe-dynamics of the uncontrolled system during optimal transport should reflect in the optimal transport cost. This cost,  $\tilde{W}$ , decreases rapidly as the time-horizon  $t_f$  is increased, as shown in Fig. 8. Hence, the optimal transport discovers the efficient paths in this chaotic system, where ‘going with the flow’ is the best option.

### 4.3 Optimal Transport for Unicycle Model

Finally, we consider optimal transport in a three-dimensional non-holonomic system, called the ‘unicycle’ model. This system is a toy model for vehicle kinematics, and is used extensively in vehicle path planning and control [77, 78]. The states are cartesian coordinates  $(x, y) \in \mathbf{R}^2$ , and orientation  $\theta \in \mathbf{S}^1$  of the unicycle. The system equations are given by,

$$\dot{x} = u_2 \cos \theta, \tag{64a}$$

$$\dot{y} = u_2 \sin \theta, \tag{64b}$$

$$\dot{\theta} = u_1, \tag{64c}$$

where  $u_1$  is the steering speed, and  $u_2$  is the translation speed. The optimal control problem has been studied for various cost functions, and endpoint conditions [79, 80, 81].

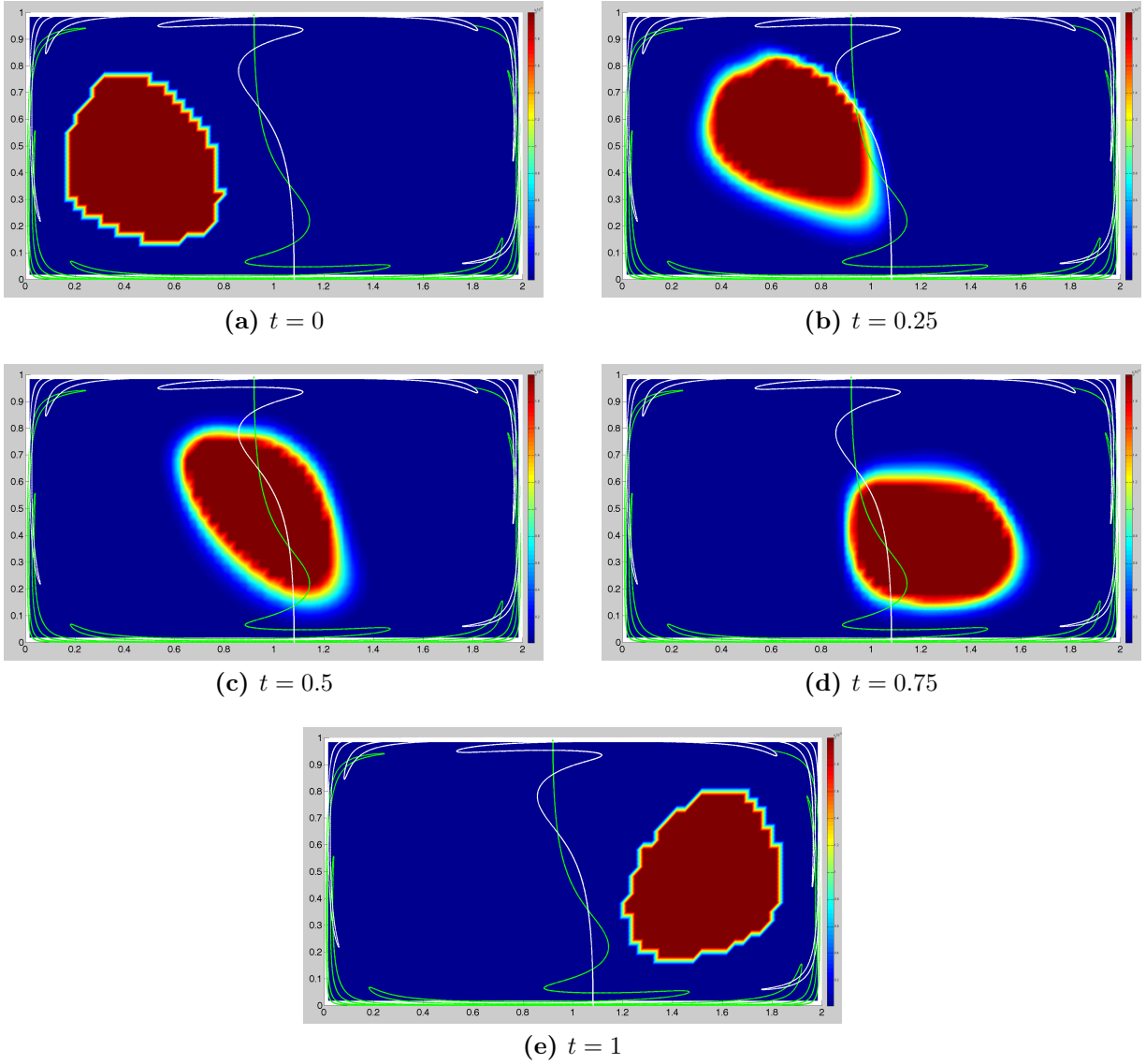


**Figure 6:** Optimal transport in the periodic double gyre system (Eqs.(63a-63b)) between measures shown in (a) and (e) for  $t_f = 1$ . The parameters are  $m = 1800, k = 40$ .

The techniques from geometric mechanics, specifically Lie-Poisson reduction [66], have been successfully used to reduce the optimal control problem to a three-dimensional non-canonical Hamiltonian system. For this three-dimensional system, two conserved quantities can be found, and hence, the optimal controls  $(u_1(t), u_2(t))$  can be solved explicitly in terms of Jacobi elliptic functions.

To study the optimal transport problem for the unicycle model, take the control cost to be quadratic, i.e.  $d(z_1, z_2) = \inf_{\mathbb{U}_{z_1}^{z_2}} \int_0^1 \sqrt{u_1^2 + u_2^2} dt$ . We compute optimal transport solutions for two scenarios. In the first case,  $\mu_0$  is chosen to be a measure supported on box containing  $(0, 0.5, 0)$ , and  $\mu_1$  is chosen to be uniform measure supported on the union of boxes containing

$(1, 0, 0)$  and  $(1, 1, 0)$ . In the second case,  $\mu_0$  is chosen to be a measure supported on box containing  $(0, 0.5, 0)$ , and  $\mu_1$  is chosen to be a uniform measure supported on the union of boxes containing  $(1, 1, \frac{\pi}{2})$  and  $(1, 0, \frac{3\pi}{2})$ . The initial and final measures for the two cases are depicted in Fig 9. The optimal transport solution for the first case is shown in Fig. 10. Since the final orientation is prescribed to be along the  $x$ -axis, this leads to a splitting of the measure half-way in the transport, and steering of the two halves horizontally to their final positions. The optimal transport solution for the second case is shown in Fig. 11. The solution in this case is qualitatively different from the first case. The two halves split and then move vertically towards final positions.

## 5 Conclusions and Future Directions

A set-oriented graph-based computational framework for continuous-time optimal transport over nonlinear dynamical systems has been developed. In the control systems setting, this framework generalizes the concept of optimal transport on graphs from that of a single integrator to control-affine nonlinear systems. This is accomplished by exploiting recent work on set-oriented infinitesimal generator approach for nonlinear dynamical systems. The controllability of measures over graphs is related to the connectivity of the ‘controlled’ graph, and is proved to be a consequence of controllability of the underlying control system. This work connects set-oriented operator-theoretic methods in dynamical systems with optimal mass transportation theory, and opens up new directions in design of efficient feedback control strategies for nonlinear multi-agent and swarm systems operating in nonlinear ambient flow fields.

Application of our set-oriented framework to larger domains, longer time-horizons and/or higher dimensional systems will require improvement in computational efficiency. Using efficient phase space discretization techniques, such as those employed in GAIO [18], one can hope to improve the efficiency of the resulting optimal transport algorithms, and apply the framework to higher dimensional dynamical systems. Graph pruning algorithms can be employed to remove edges which are not likely to be used [82].

Solutions to the optimal transport problem in the double-gyre system elucidate the role played by invariant manifolds, lobe-dynamics and almost-invariant sets in efficient transport of phase-space distributions. While it is known that invariant manifolds and lobes act as low-energy ‘channels’ in the phase-space, our results give new qualitative and quantitative information about their role in problems of transport of distributions or swarms of agents. Application of this framework to more complicated arbitrary time-varying flows should provide similar insights into the role of Lagrangian coherent structures and coherent sets. This can lead to development of efficient swarm planning and control strategies for realistic applications in ocean and air-borne systems. Moreover, using our framework, the relative importance of such objects can be studied for different types of controls.

Furthermore, recent methods in obtaining Lagrangian coherent structures and coherent sets in finite-time non-autonomous systems have used variational formulations of transport under nonlinear dynamics [3] or dynamic versions of the Laplacian [83]. It would be fruit-

ful to develop connections of these formulations with optimal mass transportation theory, extending the connections already identified in the Hamiltonian dynamics case [47]. For instance, one could define a controlled version of almost-invariant sets or coherent sets, by defining a control dynamic Laplacian, analogous to the control infinitesimal-generators as developed in the current work, or control Lyapunov measures developed in Ref. [39].

Connections with work in the closely related area of occupation measures [42] and Lyapunov measures [39] also need to be explored, especially in context of obtaining feedback control laws from the control laws obtained from optimal transport solutions. The feedback control laws constructed as solutions to the optimal transport problem guide the measure along shortest paths corresponding to solutions of the corresponding sub-Riemannian problem. Hence, it needs to be explored in what sense these laws can be used for feedback stabilization of an individual control-affine system. Moreover, the numerical approach in the current paper could also be adapted to construct time-independent feedback control laws for such systems.

## 6 Acknowledgements

We thank Matthias Kowski, Uroš Kalabič and Udit Halder for helpful discussions on geometric control theory.



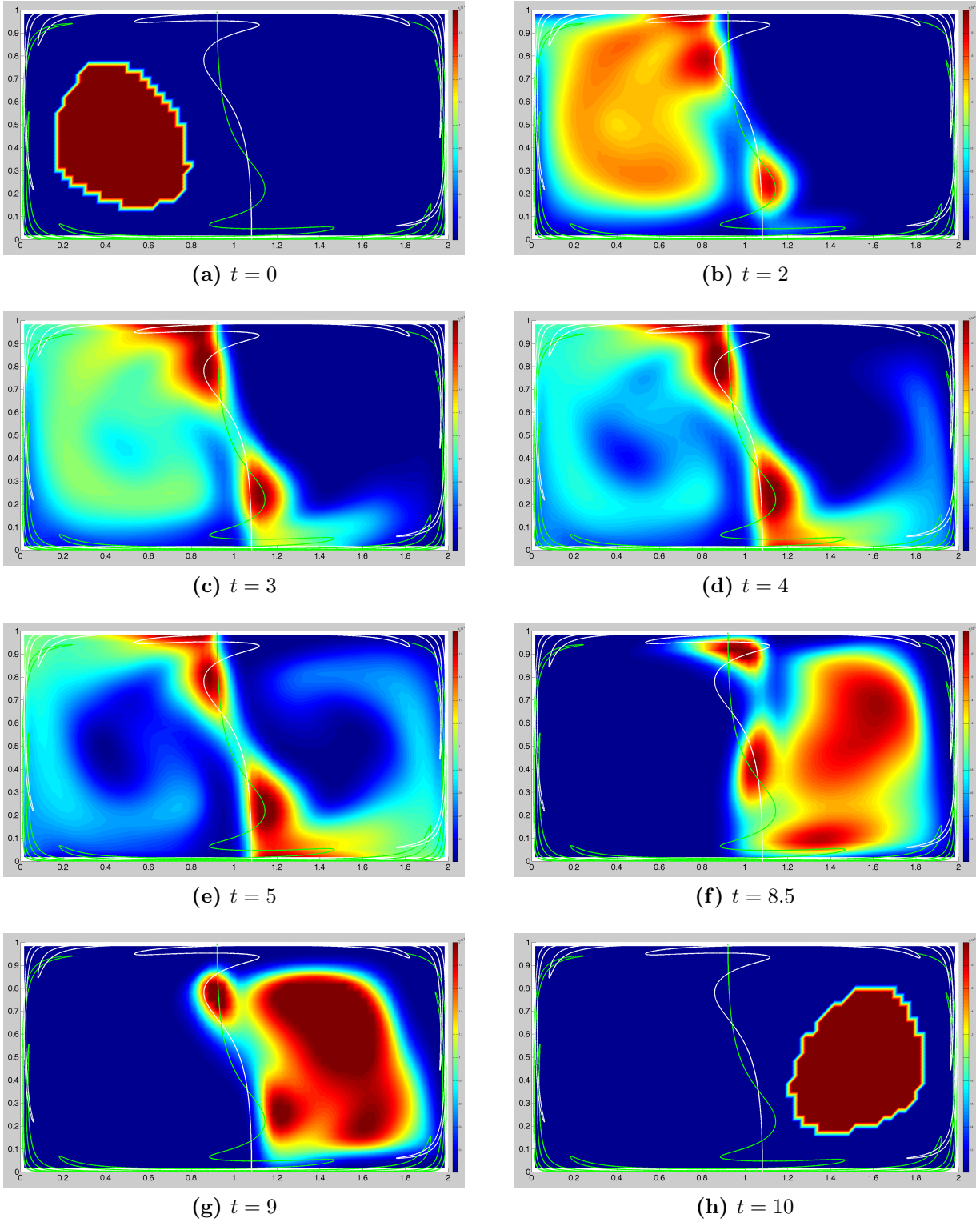


**Figure 7:** Optimal transport in the periodic double gyre system between measures shown in (a) and (h) for  $t_f = 10$ . The optimal transport solution shows a quantization phenomenon. Ten ‘packets’ are transported by lobe-dynamics from the left side to the right side of the domain. (b)-(e) The transport of third packet to right side via the sequence  $F^{-1}(A) \rightarrow A \rightarrow F(A) \rightarrow F^2(A)$ . (f)-(g) The last packet gets transported to the right side. Animation available at: <https://www.youtube.com/watch?v=Pu7sCkpm4RY>

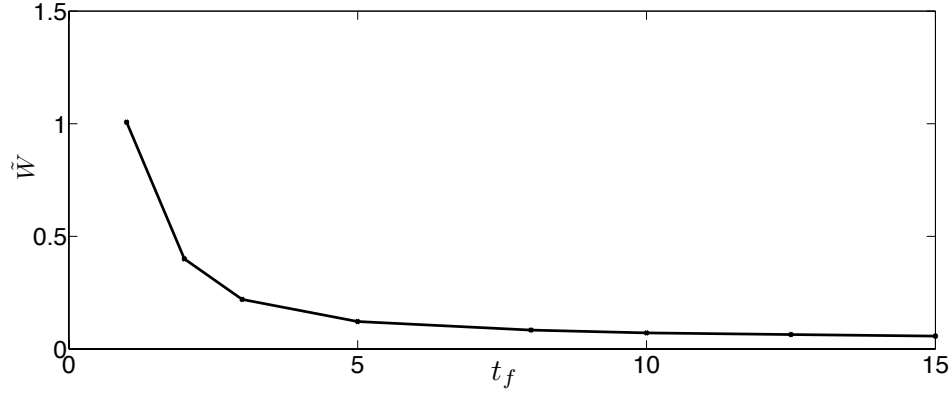


**Figure 8:** The cost of optimal transport between two measures supported on two AIS for the double-gyre system, as a function of time-horizon of the problem.

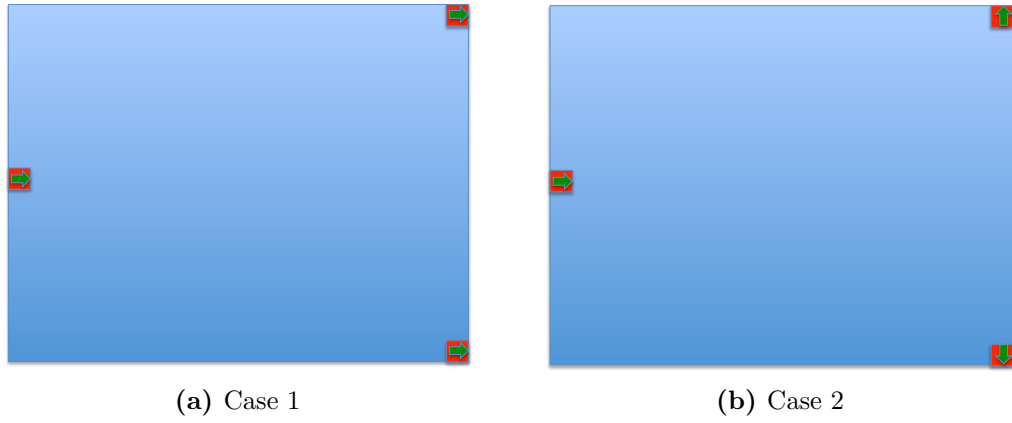


**Figure 9:** Initial and final measures shown on  $(x, y)$  plane for two cases of optimal transport in the unicycle model. The green arrows indicate the third coordinate  $\theta$ . (a)  $\mu_0$  is supported on  $(0, 0.5, 0)$ ,  $\mu_1$  is supported on  $(1, 0, 0)$  and  $(1, 1, 0)$ . (b)  $\mu_0$  is supported on  $(0, 0.5, 0)$ ,  $\mu_1$  is supported on  $(1, 0, \frac{3\pi}{2})$  and  $(1, 1, \frac{\pi}{2})$ .

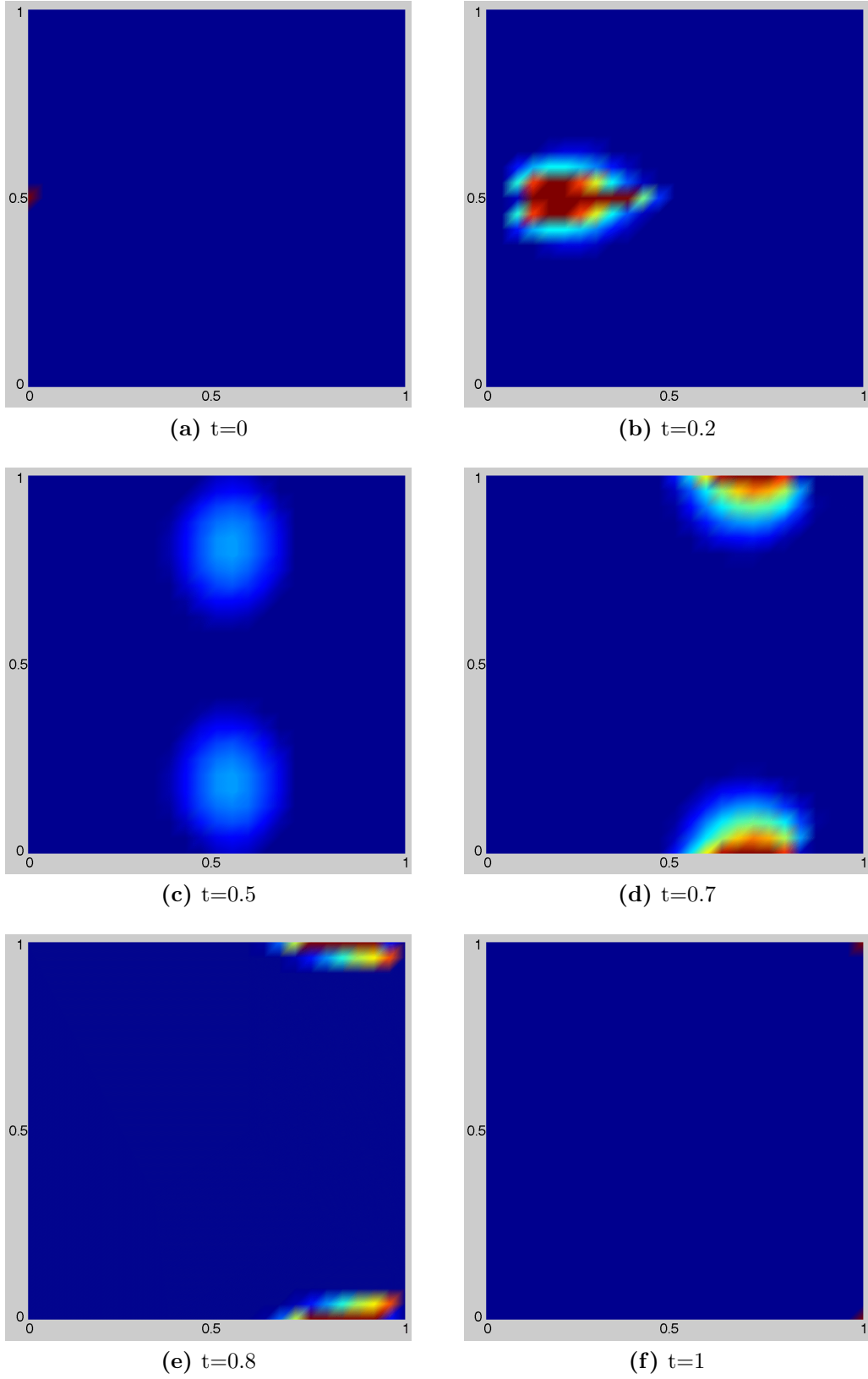


**Figure 10:** The optimal transport solution of unicycle model shown in the  $x - y$  plane for case 1. The grid size is  $m = 25^3$ , and  $k = 20$ .

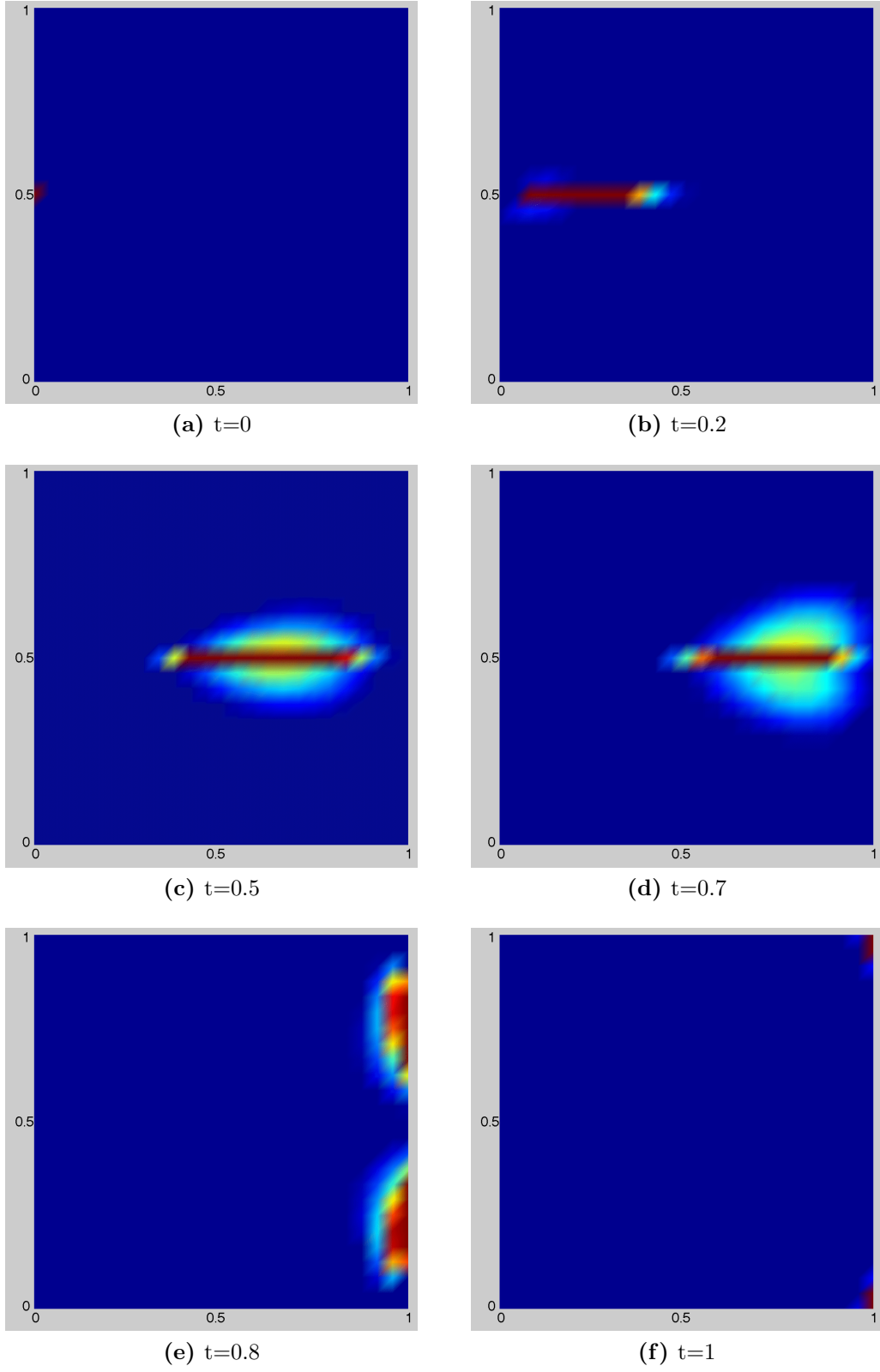


**Figure 11:** The optimal transport solution of unicycle model shown in the  $x - y$  plane for case 2. The grid size is  $m = 25^3$ , and  $k = 20$ .

## References

- [1] H. Poincaré, Les méthodes nouvelles de la mécanique céleste: Méthodes de MM. Newcomb, Glydén, Lindstedt et Bohlin. 1893, Vol. 2, Gauthier-Villars it fils, 1893.
- [2] S. Wiggins, Chaotic transport in dynamical systems, Vol. 2, Springer Science & Business Media, 2013.
- [3] G. Haller, Lagrangian coherent structures, *Annual Review of Fluid Mechanics* 47 (2015) 137–162.
- [4] J. M. Ottino, S. Wiggins, Introduction: mixing in microfluidics, *Philosophical Transactions: Mathematical, Physical and Engineering Sciences* (2004) 923–935.
- [5] S. Wiggins, J. M. Ottino, Foundations of chaotic mixing, *Philosophical Transactions of the Royal Society of London A: Mathematical, Physical and Engineering Sciences* 362 (1818) (2004) 937–970.
- [6] W. Koon, M. Lo, J. Marsden, S. Ross, *Dynamical Systems, the Three-Body Problem and Space Mission Design*, Marsden Books, 2008.
- [7] J. D. Meiss, Symplectic maps, variational principles, and transport, *Rev. Mod. Phys.* 64 (1992) 795–848.
- [8] C. Senatore, S. D. Ross, Fuel-efficient navigation in complex flows, in: 2008 American Control Conference, IEEE, 2008, pp. 1244–1248.
- [9] J. Sabuco, M. A. Sanjuán, J. A. Yorke, Dynamics of partial control, *Chaos* 22 (2012) 047507.
- [10] U. Vaidya, I. Mezić, Controllability for a class of area-preserving twist maps, *Physica D: Nonlinear Phenomena* 189 (3) (2004) 234–246.
- [11] D. Vainchtein, A. Neishtadt, I. Mezic, On passage through resonances in volume-preserving systems, *Chaos: An Interdisciplinary Journal of Nonlinear Science* 16 (4) (2006) 043123.
- [12] R. Gilmore, Topological analysis of chaotic dynamical systems, *Reviews of Modern Physics* 70 (4) (1998) 1455.
- [13] P. Boyland, H. Aref, M. Stremler, Topological fluid mechanics of stirring, *Journal of Fluid Mechanics* 362 (2000) 1019–1036.
- [14] J.-L. Thiffeault, M. D. Finn, Topology, braids and mixing in fluids, *Philosophical Transactions of the Royal Society of London A: Mathematical, Physical and Engineering Sciences* 364 (1849) (2006) 3251–3266.
- [15] M. D. Finn, J.-L. Thiffeault, Topological optimization of rod-stirring devices, *SIAM review* 53 (4) (2011) 723–743.
- [16] A. Lasota, M. Mackey, *Chaos, Fractals and Noise*, Springer-Verlag, New York, 1994.
- [17] M. Dellnitz, O. Junge, On the approximation of complicated dynamical behavior, *SIAM Journal on Numerical Analysis* 36 (1998) 491–515.
- [18] M. Dellnitz, G. Froyland, O. Junge, The algorithms behind GAIO – set oriented numerical methods for dynamical systems, in: B. Fiedler (Ed.), *Ergodic Theory, Analysis, and Efficient Simulation of Dynamical Systems*, Springer, Berlin-Heidelberg-New York, 2001, pp. 145–174.
- [19] M. Budišić, R. Mohr, I. Mezić, Applied koopmanism, *Chaos: An Interdisciplinary Journal of Nonlinear Science* 22 (4) (2012) 047510.
- [20] E. M. Bollt, N. Santitissadeekorn, *Applied and Computational Measurable Dynamics*, Vol. 18, SIAM, 2013.

- [21] I. Mezic, Analysis of fluid flows via spectral properties of the koopman operator, *Annual Review of Fluid Mechanics* 45 (2013) 357–378.
- [22] M. Dellnitz, O. Junge, W. S. Koon, F. Lekien, M. W. Lo, J. E. Marsden, K. Padberg, R. Preis, S. D. Ross, B. Thiere, Transport in dynamical astronomy and multibody problems, *Int. J. Bifurc. Chaos* 15 (2005) 699–727.
- [23] G. Froyland, K. Padberg, Almost-invariant sets and invariant manifolds – connecting probabilistic and geometric descriptions of coherent structures in flows, *Physica D* 238(16) (2009) 1507–1523.
- [24] P. Tallapragada, S. D. Ross, A set oriented definition of finite-time lyapunov exponents and coherent sets, *Communications in Nonlinear Science and Numerical Simulation* 18 (5) (2013) 1106–1126.
- [25] P. Grover, S. D. Ross, M. A. Stremler, P. Kumar, Topological chaos, braiding and bifurcation of almost-cyclic sets, *Chaos: An Interdisciplinary Journal of Nonlinear Science* 22 (4) (2012) 043135.
- [26] M. A. Stremler, S. D. Ross, P. Grover, P. Kumar, Topological chaos and periodic braiding of almost-cyclic sets, *Physical review letters* 106 (11) (2011) 114101.
- [27] G. Froyland, M. Dellnitz, Detecting and locating near-optimal almost-invariant sets and cycles, *SIAM Journal on Scientific Computing* 24 (2003) 1839–1863.
- [28] G. Froyland, N. Santitissadeekorn, A. Monahan, Transport in time-dependent dynamical systems: Finite-time coherent sets, *Chaos* 20 (2010) 043116.
- [29] C. Villani, *Topics in optimal transportation*, no. 58, American Mathematical Society, 2003.
- [30] A. Ghosh, P. Fischer, Controlled propulsion of artificial magnetic nanostructured propellers, *Nano letters* 9 (6) (2009) 2243–2245.
- [31] U. K. Cheang, K. Lee, A. A. Julius, M. J. Kim, Multiple-robot drug delivery strategy through coordinated teams of microswimmers, *Applied physics letters* 105 (8) (2014) 083705.
- [32] K. E. Peyer, L. Zhang, B. J. Nelson, Bio-inspired magnetic swimming microrobots for biomedical applications, *Nanoscale* 5 (4) (2013) 1259–1272.
- [33] K. Elamvazhuthi, S. Berman, Optimal control of stochastic coverage strategies for robotic swarms, in: 2015 IEEE International Conference on Robotics and Automation (ICRA), IEEE, 2015, pp. 1822–1829.
- [34] R. Wood, R. Nagpal, G.-Y. Wei, Flight of the robobees, *Scientific American* 308 (3) (2013) 60–65.
- [35] P. Lermusiaux, T. Lolla, P. Haley Jr, K. Yigit, M. Ueckermann, T. Sondergaard, W. Leslie, Science of autonomy: Time-optimal path planning and adaptive sampling for swarms of ocean vehicles, *Springer Handbook of Ocean Engineering: Autonomous Ocean Vehicles, Subsystems and Control*.
- [36] O. Junge, H. M. Osinga, A set oriented approach to global optimal control, *ESAIM: Control, optimisation and calculus of variations* 10 (2) (2004) 259–270.
- [37] S. D. Ross, S. Jerg, O. Junge, Optimal capture trajectories using multiple gravity assists, *Communications in Nonlinear Science and Numerical Simulations* 14 (12) (2009) 4168–4175.
- [38] S. Jerg, O. Junge, M. Post, Global optimal feedbacks for stochastic quantized nonlinear event systems.
- [39] U. Vaidya, P. G. Mehta, Lyapunov measure for almost everywhere stability, *IEEE Transactions on Automatic Control* 53 (1) (2008) 307–323.
- [40] U. Vaidya, P. G. Mehta, U. V. Shanbhag, Nonlinear stabilization via control lyapunov measure, *IEEE Transactions on Automatic Control* 55 (6) (2010) 1314–1328.
- [41] A. Raghunathan, U. Vaidya, Optimal stabilization using lyapunov measures, *IEEE Transactions on Automatic Control* 59 (5) (2014) 1316–1321.

- [42] J. B. Lasserre, D. Henrion, C. Prieur, E. Trélat, Nonlinear optimal control via occupation measures and lmi-relaxations, *SIAM Journal on Control and Optimization* 47 (4) (2008) 1643–1666.
- [43] G. Froyland, C. González-Tokman, T. M. Watson, Optimal mixing enhancement by local perturbation, *SIAM Review* 58(3) (2016) 494–513.
- [44] G. Froyland, N. Santitissadeekorn, Optimal mixing enhancement, arXiv preprint arXiv:1610.01651.
- [45] J. Maas, Gradient flows of the entropy for finite markov chains, *Journal of Functional Analysis* 261 (8) (2011) 2250–2292.
- [46] A. Figalli, L. Rifford, Mass transportation on sub-riemannian manifolds, *Geometric And Functional Analysis* 20 (1) (2010) 124–159.
- [47] P. Bernard, B. Buffoni, Optimal mass transportation and mather theory, arXiv preprint math/0412299.
- [48] L. Ambrosio, N. Gigli, G. Savaré, Gradient flows: in metric spaces and in the space of probability measures, Springer Science & Business Media, 2008.
- [49] A. Hindawi, J.-B. Pomet, L. Rifford, Mass transportation with LQ cost functions, *Acta applicandae mathematicae* 113 (2) (2011) 215–229.
- [50] Y. Chen, T. T. Georgiou, M. Pavon, Optimal transport over a linear dynamical system, *IEEE Transactions on Automatic Control* 62 (5) (2017) 2137–2152.
- [51] Y. Chen, T. T. Georgiou, M. Pavon, On the relation between optimal transport and schrödinger bridges: A stochastic control viewpoint, *Journal of Optimization Theory and Applications* 169 (2) (2016) 671–691.
- [52] P. Grover, K. Elamvazhuthi, Optimal perturbations for nonlinear systems using graph-based optimal transport, arXiv preprint arXiv:1611.06278.
- [53] J.-D. Benamou, Y. Brenier, A computational fluid mechanics solution to the monge-kantorovich mass transfer problem, *Numerische Mathematik* 84 (3) (2000) 375–393.
- [54] A. Agrachev, P. Lee, Optimal transportation under nonholonomic constraints, *Transactions of the American Mathematical Society* 361 (11) (2009) 6019–6047.
- [55] L. Rifford, B. (centre), Sub-Riemannian geometry and optimal transport, Springer, 2014.
- [56] S. M. Ulam, Problems in modern mathematics, Courier Corporation, 2004.
- [57] K.-J. Engel, R. Nagel, One-parameter semigroups for linear evolution equations, Vol. 194, Springer Science & Business Media, 1999.
- [58] H. O. Fattorini, The cauchy problem, Vol. 13517, Cambridge University Press, 1984.
- [59] G. Froyland, O. Junge, P. Koltai, Estimating long-term behavior of flows without trajectory integration: The infinitesimal generator approach, *SIAM Journal on Numerical Analysis* 51 (1) (2013) 223–247.
- [60] S. Berman, Á. Halász, M. A. Hsieh, V. Kumar, Optimized stochastic policies for task allocation in swarms of robots, *IEEE Transactions on Robotics* 25 (4) (2009) 927–937.
- [61] A. Chapman, M. Mesbahi, Advection on graphs, in: 2011 50th IEEE Conference on Decision and Control and European Control Conference, IEEE, 2011, pp. 1461–1466.
- [62] N. Gigli, J. Maas, Gromov–hausdorff convergence of discrete transportation metrics, *SIAM Journal on Mathematical Analysis* 45 (2) (2013) 879–899.
- [63] A. Mielke, Geodesic convexity of the relative entropy in reversible markov chains, *Calculus of Variations and Partial Differential Equations* (2013) 1–31.

- [64] J. Solomon, R. Rustamov, L. Guibas, A. Butscher, Continuous-flow graph transportation distances, arXiv preprint arXiv:1603.06927.
- [65] D. L. Elliott, Bilinear control systems: matrices in action, Vol. 169, Springer Science & Business Media, 2009.
- [66] A. Bloch, J. Baillieul, P. Crouch, J. E. Marsden, P. S. Krishnaprasad, R. Murray, D. Zenkov, Nonholonomic mechanics and control, Vol. 24, Springer, 2003.
- [67] A. A. Agrachev, Y. Sachkov, Control theory from the geometric viewpoint, Vol. 87, Springer Science & Business Media, 2013.
- [68] H. J. Sussmann, A general theorem on local controllability, SIAM Journal on Control and Optimization 25 (1) (1987) 158–194.
- [69] K. Elamvazhuthi, V. Deshmukh, M. Kawski, S. Berman, Mean-field controllability and decentralized stabilization of markov chains, part i: Global controllability and rational feedbacks, arXiv preprint arXiv:1703.08243.
- [70] N. Papadakis, G. Peyré, E. Oudet, Optimal transport with proximal splitting, SIAM Journal on Imaging Sciences 7 (1) (2014) 212–238.
- [71] M. Grant, S. Boyd, Y. Ye, CVX: Matlab software for disciplined convex programming (2008).
- [72] B. O’Donoghue, E. Chu, N. Parikh, S. Boyd, Operator splitting for conic optimization via homogeneous self-dual embedding, arXiv preprint arXiv:1312.3039.
- [73] J. Eckstein, W. Yao, Augmented lagrangian and alternating direction methods for convex optimization: A tutorial and some illustrative computational results, RUTCOR Research Reports 32.
- [74] F. Lekien, C. Coulliette, Chaotic stirring in quasi-turbulent flows, Philosophical Transactions of the Royal Society of London A: Mathematical, Physical and Engineering Sciences 365 (1861) (2007) 3061–3084.
- [75] A. Poje, G. Haller, Geometry of cross-stream mixing in a double-gyre ocean model, Journal of physical oceanography 29 (8) (1999) 1649–1665.
- [76] S. Wiggins, The dynamical systems approach to lagrangian transport in oceanic flows, Annu. Rev. Fluid Mech. 37 (2005) 295–328.
- [77] R. M. Murray, S. S. Sastry, Nonholonomic motion planning: Steering using sinusoids, IEEE Transactions on Automatic Control 38 (5) (1993) 700–716.
- [78] M. Aicardi, G. Casalino, A. Bicchi, A. Balestrino, Closed loop steering of unicycle like vehicles via lyapunov techniques, IEEE Robotics & Automation Magazine 2 (1) (1995) 27–35.
- [79] P. S. Krishnaprasad, Optimal control and poisson reduction, Tech. rep., DTIC Document (1993).
- [80] E. Kirillova, K. Spindler, Optimal control of a vehicle during parking, in: 2004 IFAC Symposium on Nonlinear Control Systems (NOLCOS), pp. 1205–1210.
- [81] E. W. Justh, P. Krishnaprasad, Optimality, reduction and collective motion, in: Proc. R. Soc. A, Vol. 471, The Royal Society, 2015, p. 20140606.
- [82] D. D. Harabor, A. Grastien, et al., Online graph pruning for pathfinding on grid maps., in: AAAI, 2011.
- [83] G. Froyland, Dynamic isoperimetry and the geometry of lagrangian coherent structures, Nonlinearity 28 (10) (2015) 3587.